UNIVERSITÀ DEGLI STUDI DI BRESCIA

Dipartimento di Medicina Molecolare e Traslazionale

UNIVERSITÀ
DEGLI STUDI
DI BRESCIA

DOTTORATO DI RICERCA IN

Genetica Molecolare, Biotecnologie e Medicina Sperimentale

settore scientifico disciplinare

BIO/13

CICLO XXXV

TITOLO TESI

Unravelling the role of CYFIP2 and R87C mutation in "*in vitro*" neurodevelopment

RELATORE: Prof. Alessandro Barbon

DOTTORANDA: Elona Ndoj

Anno Accademico 2023/2024

INDEX

LIST OF ABBREVIATIONS

Abbreviation	Definition
ABI2	Arg-Binding Protein Interactor 2
ADAR	Adenosine Deaminase Acting on RNA
AGO2	Argonaute RISC Catalytic Component 2
ARC	Activity-regulated cytoskeleton-associated protein
Arp 2/3	Actin Related Protein 2/3
ASD	Autism spectrum disorder
C57BL/6	C57 black 6 mouse
CaMKII	Ca2+/calmodulin-dependent protein kinase II
Cas9	CRISPR associated protein 9
CD4+	CD4 T lymphocytes
CDS	Coding Sequence
CNS	Central Nervous System
CRISPR	Clustered Regularly Interspaced Short Palindromic Repeats
cryo-EM	cryo-electron microscopy
CYFIP1	Cytoplasmic FMRP Interacting Protein 1
CYFIP2	Cytoplasmic FMRP Interacting Protein 2
DIV	Day *In Vitro*
DSB	Double Strand Break
E2F1	E2F Transcription Factor 1
EIEE	Early Infanitle Epileptic Encephalopathy
ECS	Editing Complementary Sequence

eIF4E	Eukaryotic translation initiation factor 4E
FMRP	Fragile X Messenger Ribonucleoprotein
FXR1P	Fragile X related protein 1
FXR1P	Fragile X related protein 2
FXS	Fragile X syndrome
GTPase	GTP-binding proteins
ID	Intellectual disability
IGFBP7	Insulin Like Growth Factor Binding Protein 7
KD	Gene *Knock-Down*
kDa	Kilo Dalton
KI	*Gene Knock-In*
KO	*Gene Knock-Out*
MAP1B	Microtubule Associated Protein 1B
miRNA	Micro RNA
MOI	Multiplicity Of Infection
mTOR	Mechanistic Target Of Rapamycin Kinase
NCKAP1	NCK Associated Protein 1
NPFs	Nucleation-promoting factors
Nt	Nucleotide
P53	Tumor protein P53
PFA	Paraformaldehyde
PDB	Protein Data Bank
PIR121	P53-Inducible Protein 121
PUM1	Pumilio1
RAC1	Ras-related C3 botulinum toxin substrate 1
RGCs	Retinal glial cells
RHO	Ras Homologous protein family
RT	Room Temperature

SCAR	Suppressor of cAMP Receptor
scRNAseq	Single-cell RNA sequencing
sgRNA	Single Guide RNA
SRA-1	Steroid Receptor RNA Activator 1
UTRs	UnTranslated Region
WASP	Wiskott–Aldrich syndrome protein
WAVE	WASP family Verprolin homolog
WCA	WH2-central-acidic motif
WH2 domain	WASP-Homology 2 domain
WRC	Wave Regulatory Complex
WT	Wild Type

ABSTRACT

Unravelling the role of CYFIP2 and R87C mutation in "*in vitro*" neurodevelopment:

Cytoplasmic FMRP Interacting Protein 2 (CYFIP2) è una proteina originariamente identificata come componente del Wave Regulatory Complex (WRC) e come interattore di Fragile-X Messenger Ribonucleoprotein (FMRP). Ha un importante ruolo nelle dinamiche dell'actina ~~che a loro~~ volta sono implicate in una serie di processi biologici nella fisiologia cellulare. Le dinamiche dell'actina sono infatti, implicate sia nella divisione e motilità cellulare, sia nella formazione di strutture specializzate come spine oppure cono di crescita nell'assone nei neuroni. Tutto ciò conferisce a questa proteina un ruolo ampio in una serie di processi fisiologici. Nella sequenza genica che codifica questa proteina sono state riscontrate un serie di mutazioni associate all'insorgenza di diverse patologie neurologiche. Nel 2018 Nakashima e colleghi hanno scoperto in particolare tre mutazioni de-novo (R87C, R87L, R87P) in questa sequenza, che sono state riscontrate in una serie di patologie di neuro- sviluppo come le Encefalopatie Infantili ad Esordio Precoce, nonché la West Sindrome. Tra tutte tre le mutazioni l'oggetto del nostro studio è stata la mutazione R87C la quale conferisce la prognosi peggiore nei pazienti ed è anche la più frequente.

L'obiettivo di questa tesi è stato la caratterizzazione di un serie di parametri morfologici/funzionali in diversi modelli cellulari, che possono essere alterati dalla mutazione R87C.

I nostri risultati hanno dimostrato inizialmente che la proteina mutata ha un'espressione ridotta rispetto a WT, e che questa ridotta espressione potrebbe essere dovuta a un aumento di degradazione.

Successivamente, per approfondire il ruolo della proteina CYFIP2 e anche quella della mutazione di R87C, abbiamo usato un modello cellulare rappresentato da una linea di neuroblastoma SH-SY5Y. Inizialmente abbiamo eliminato il gene CYFIP2 utilizzando la tecnica CRISPR-Cas9, generando una linea cellulare KO per il gene di interesse. Successivamente, abbiamo sovra espresso sia CYFIP2 che

R87C nelle linee KO tramite trasduzione lentivirale. La sovra espressione di entrambe le varianti ha ripristinato il fenotipo morfologico osservato nelle cellule KO. I risultati in questo modello evidenziano differenze morfologiche/funzionali, che riguardano alcuni parametri che sono conseguenza di dinamiche dell'actina e della riorganizzazione del citoscheletro. Questi dati suggeriscono che la proteina mutata altera le dinamiche dell'actina. Poiché la proteina CYFIP2 è espressa principalmente nei neuroni, abbiamo indagato il ruolo della mutazione R87C durante lo sviluppo neuronale. A tal fine, abbiamo utilizzato un consolidato modello di differenziamento neuronale in cellule SH-SY5Y, basato sull'uso di terreno arricchito con acido retinoico (RA) e del fattore di crescita neuronale BDNF, che inducono la differenziazione delle cellule con morfologia simil-neuronale. I nostri risultati dimostrano chiaramente che le cellule prive del gene CYFIP2 (KO) perdono la capacità di sviluppare una tipica morfologia simil-neuronale dopo il differenziamento, mentre la sovra-espressione della proteina CYFIP2 ripristina tale capacità di differenziare. Invece la mutazione impedisce in qualche modo questo processo, infatti le cellule mutate mostrano una lunghezza di neurite inferiore o nulla se paragonate con le cellule esprimenti CYFIP2.

Per approfondire il nostro studio, abbiamo scelto di utilizzare colture neuronali primarie di roditori. L'espressione endogena di CYFIP1 e CYFIP2 è stata ridotta mediante l'uso di shRNA specifici, e le colture cellulari sono state trasdotte con vettori lentivirali che esprimono sia la proteina CYFIP2 che la mutazione R87C. Durante il processo di maturazione neuronale, abbiamo esaminato parametri morfologici relativi allo sviluppo degli assoni. Abbiamo osservato una differenza statisticamente significativa tra i neuroni che esprimono la mutazione R87C e quelli che esprimono la proteina CYFIP2, in termini di numero di ramificazioni, lunghezza totale e indice di complessità degli assoni analizzati. In aggiunta, abbiamo utilizzato il nostro modello di colture primarie ippocampali per indagare se la mutazione possa essere coinvolta nel processo di sinaptogenesi. I nostri risultati rivelano che la frequenza delle spine sinaptiche è drasticamente ridotta nelle cellule che esprimono la proteina mutata.

Questi dati valutati nel loro insieme suggeriscono che la patogenicità di questa proteina mutata potrebbe essere data da diversi fattori. In primis la riduzione della sua espressione dovuta alla degradazione. In secondo luogo, la modulazione di processi implicati nelle dinamiche dell'actina che impattano la morfologia cellulare nonché differenziamento e spinogensi. Tuttavia, i meccanismi di queste alterazioni osservate rimangono ignote.

1. INTRODUCTION

1.1 Actin dynamics

Actin is a globular protein, with a conserved structure across eukaryotes. It consists of a single polypeptide chain folded into a compact globular shape. Actin monomers (G-actin) have a molecular weight of approximately 42 kDa. Actin monomers polymerize into long, filamentous structures called F-actin (Figure 1.1). Polymerization occurs through the addition of G-actin monomers to the ends of existing filaments. The polymerization process is regulated by the availability of ATP and the presence of actin-binding proteins. Actin dynamics play a pivotal role in numerous cellular processes, contributing to cell shape, movement, division, and intracellular transport (Blanchoin *et al.*, 2014). Actin filaments, composed of globular actin monomers polymerized into long chains, undergo constant turnover through processes like polymerization, depolymerization, and filament bundling. Actin polymerization, driven by the hydrolysis of ATP, generates force for cell motility, including cell crawling and muscle contraction. Actin-binding proteins regulate filament assembly and disassembly, controlling the spatiotemporal organization of actin networks. Moreover, actin dynamics participate in intracellular trafficking, facilitating the movement of organelles and vesicles along cytoskeletal tracks (Schaks, Giannone and Rottner, 2019). Overall, the dynamic properties of actin filaments orchestrate a wide array of cellular activities, essential for cell function and tissue homeostasis.

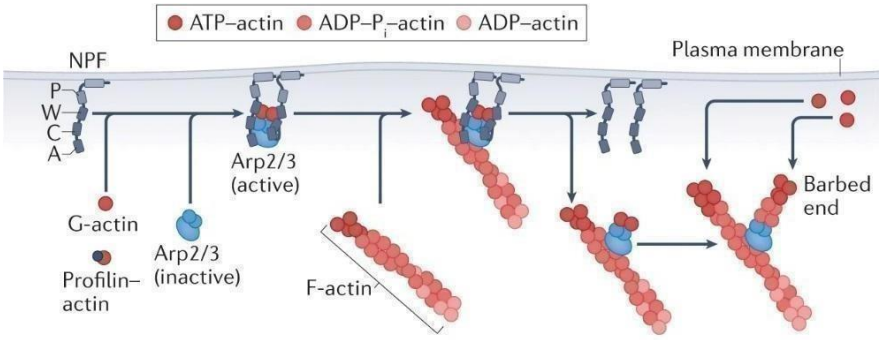

Figure 1.1: The image illustrates the process by which Nucleation-Promoting Factors (NPFs) activate the Arp2/3 complex to generate branched actin filaments. NPFs utilize specific domains to recruit actin monomers and interact with the Arp2/3 complex. This activation allows Arp2/3 to attach to an existing actin filament and promote the growth of a new, branched filament. Adapted from (Lappalainen *et al.*, 2022)

1.2 Actin based protrusion types

Cell migration is a crucial function in cell life and most of the time this function relies in actin dynamics specifically in the capacity to assembly and disassembly of actin filament. This process is highly regulated by a series of signaling cascades actively involved. The end point of this process is the organization of the cell structure in order to adapt to various stimuli in time and space such as the need to move or to create physical contact with other cells as well as to divide. Indeed, actin dynamics are crucial for the formation of specialized structures like lamellipodia, filopodia and blebs, essential for cell migration and sensing the extracellular environment and so on.

These three different types of protrusion can be obtained by different mechanisms that recruit a distinct arrangement of actin filaments (Fig 2). For instance, lamellipodia is a type of cell protrusion also called ruffles which is formed by continuous branching of Arp2/3 complex that is triggered by activation of WRC which in turn is activated by Rac GTPase signaling. During this process, actin polymerization generates the necessary force required to overcome membrane tension, the entire process operates independently of myosin II-driven contractility (Oakes *et al.*, 2018). The formation of lamellipodia is linked with mesenchymal migration (Schaks, Giannone and Rottner, 2019).

The other type of protrusion is filopodia in which actin filaments are organized in small assemblies, and the gaps between the separate bundles are occupied by contractile activity driven by myosin (Steffen *et al.*, 2006). Also in this case, the protrusion is given by the force generated during polymerization of actin. The third type of plasma membrane protrusion is the bleb, which, unlike lamellipodia and filopodia, does not rely on actin polymerization but rather on myosin (Charras *et al.*, 2005). Given that bleb formation is dependent on myosin II activity, it indicates that intracellular hydrostatic pressure acts as the driving force in this case (Bergert et al.,2012; Paluch and Raz, 2013). The antagonism between protrusion types is somehow regulated upstream, by activation of different signaling and effectors. For instance, axis Rac-WRC-Arp2/3 is strongly involved in lamellipodia formation while Rho-ROCK-myosin II is more involved in bleb formation and somehow antagonize the formation of lamellipodia (Bergert et al., 2012) In the other hand ROCK-myosin activation, either by Rho signaling or Cdc42 GTPases modulate the outcome signals leading to formation of blebs or filopodia respectively.

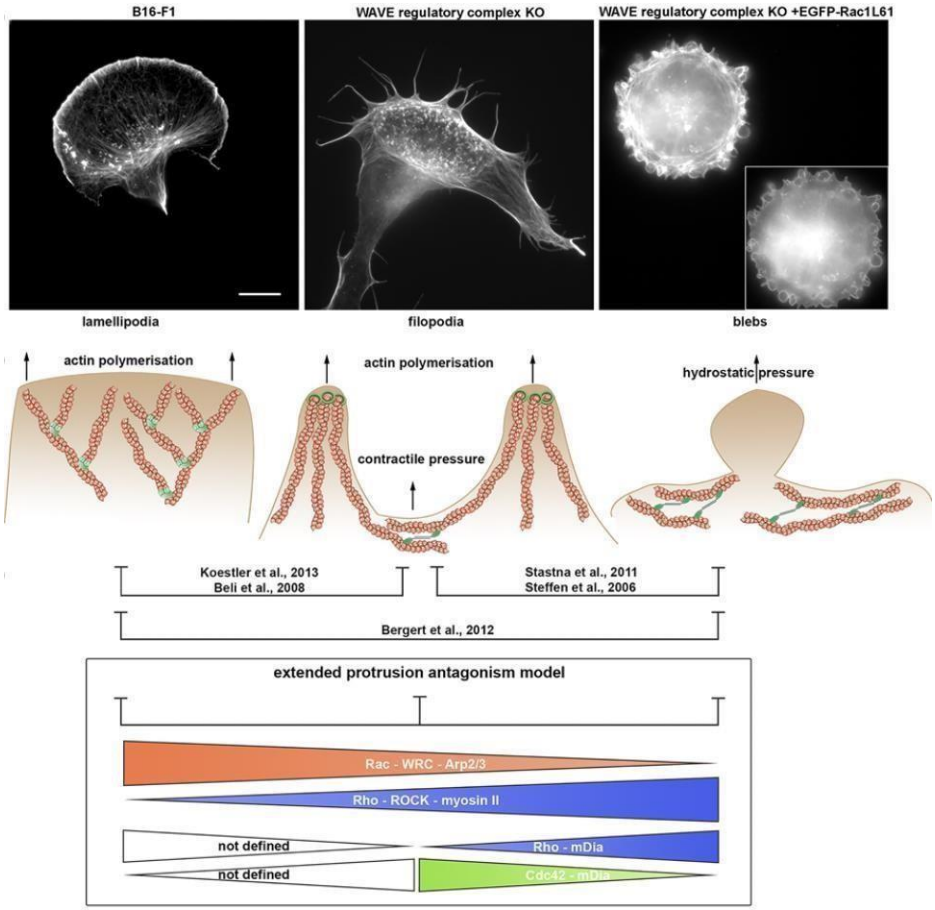

Figure 1.2: Types of actins-based protrusion and signaling involved in this process (Koestler *et al.*, 2013; Steffen *et al.*, 2013)

2.1 WAVE Regulatory Complex WRC

WAVE (WASP-family Verprolin homolog) also known as SCAR for suppressor of cAMP receptor, is one of the WASP (Wiskott-Aldrich syndrome protein) family members. WAVE operates as part of heteropentameric complex called WAVE regulatory complex (WCR) with a complessive molecular weight around 400 kDa, which has been discovered by Kirschener (Gautreau *et al.*, 2004). Since then, this complex has attracted considerable attention and has been the subject of many studies due to its significant role in various diseases as well as because of ist key function in actin remodeling. WRC is composed of five protein subunits which are conserved among species. Each subunits in vertebrate and multicellular organism display multiple ortholog for example Sra/Cyfip1 (its ortholog Pir121/Cyfip2), Nap1/Hem2 (its ortholog Hem1), Abi2 (its orthologs Abi1 and Abi3/Nesh),

HSPC300/BRICK1 and WAVE1/SCAR1 (ist orthologs WAVE2 and WAVE3). The composition of five subunits are conserved across species. The orthologs in a defined species can be exchanged in different tissues and may have specific tissue distribution. For instance, in humans CYFIP2 is mostly expressed in neuronal tissue while its ortholog is expressed in the rest of the organism. The five subunits seem to have co-exist through evolution. Another interesting feature of this complex is the importance of its fully assembled in order to exercit its function, indeed by knocking down one of the five subunits the expression of other components is reduced or totally interrupted and finally the whole complex ceases to operate.

Recent research has identified the WRC as a central hub for communication between the plasma membrane and actin across a variety of cellular functions, shedding light on several crucial mechanisms of the WRC. It is generally well established that in its resting state, the WRC remains autoinhibited in the cytosol. Numerous upstream signals, including ligand-binding proteins like GTPases, inositol phospholipids, membrane receptors, and scaffolding proteins, along with post-translational modifications such as phosphorylation and ubiquitination, often collaborate within the cell to lift this inhibition. These signals facilitate the recruitment of WASP-family proteins to specific membrane regions, where they then activate the Arp2/3 complex to drive actin polymerization (Abdul-Manan *et al.*, 1999; Rottner, Stradal and Chen, 2021) (Fig. 1.3).

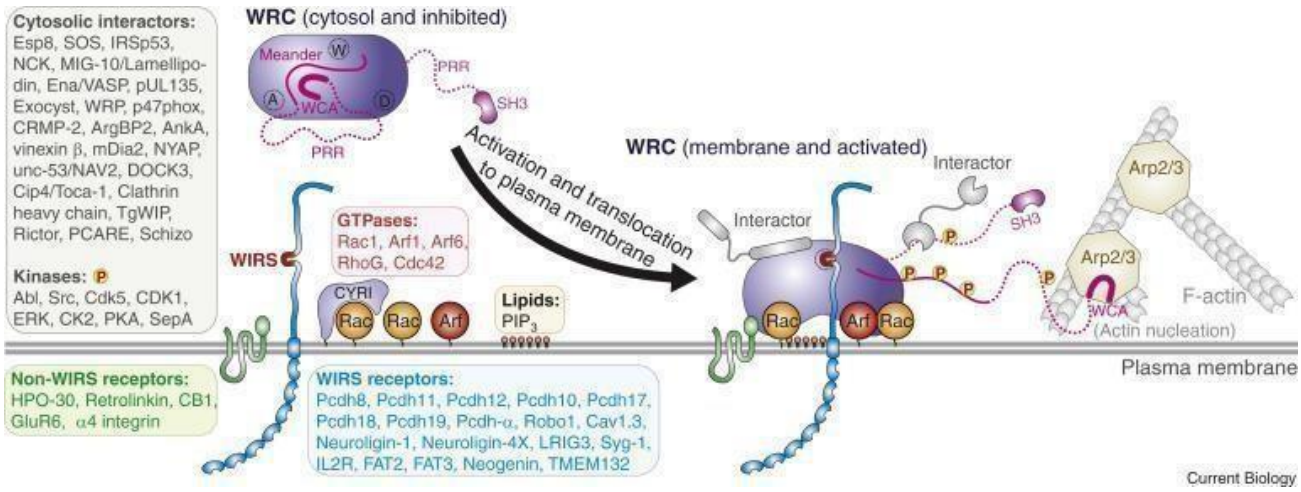

Figure 1.3: The simultaneous activation of the WRC and its movement toward the plasma membrane by numerous membrane ligands leads to the release of the WCA. This release enables WCA to bind with the Arp2/3 complex, thereby promoting actin nucleation and the formation of branching actin networks (Rottner, Stradal and Chen, 2021)

3.1 Cytoplasmic FMR1 interacting family members.

In humans the cytoplasmic FMR 1 interacting proteins consist of two main members, CYFIP1 and CYFIP2 which are evolutionarily conserved proteins, originally identified as binding partners of fragile X mental retardation protein (FMRP). Both of them, with a molecular weight of approximately 145 KDa, are involved in neuro-development and maturation as well as in several mental disorders such as autism spectrum disorders, intellectual disability, Alzheimer diseases, and lately has been found an implication also in schizophrenia. Even though they share a 95% similarity, and 88% identity (Zhang, Lee and Han, 2019), as well as shared interaction with binding partners, they act at different points in cellular processes. In the first place, they have a different expression pattern in different tissues as well as cellular type. For instance, CYFIP2 is highly expressed in brain, kidney, and lymphnodes while CYFIP1 is expressed in most human tissues. Moreover, regarding the expression pattern in the brain, CYFIP2 is mostly expressed in neuronal cells whereas CYFIP1 is expressed in non-neuronal cells such as astrocytes and glial cells. Knock down animals of CYFIP1 and CYFIP2 are not viable and show lethality at different developmental stages 9.5 days and 18.6 respectively.

CYFIP1, like CYFIP2, part of heteropentametric complex Wiskott Aldrich syndrome protein family verprolin homologous protein WAVE Regulatory complex (WRC) and plays a crucial role in actin dynamic via Arp2 and Arp3 activation. (Kage et al., 2022). In addition both CYFIP1 and CYFIP2 are actively involved in mRNA translation and transport, as well as in the control of mitochondrial function and morphology (Napoli et al., 2008; Kanellopoulos et al., 2020).

3.2 The physiological role of CYFIP1

Cytoplasmic FMR1- interaction protein 1 (CYFIP1, SRA-1, KIAA0068, SHYC or P140SRA-1) is a protein coding gene located on chromosome 15q11.2. It is composed of 34 exons and according to the UniProtKB Database (Q7L576) it may encode three isoforms generated by alternative splicing. CYFIP1 protein is a 1253 amino acid long protein with a low tissue specificity expression rate (0.15) Tau specificity score RNA (Yanai et al., 2005). Initially CYFIP1 was described as an interector of Rac1 which is a member of Rho small GTPases (Kobayashi et al., 1998). Rac 1 is involved in numerous cellular function and signaling cascades among all of them it has been implicated in CYFIP1 signaling and actin filament organization. (Kobayashi et al., 1998) Indeed WRC, which CYFIP1 is part of it, is activated by Rac GTP. This complex, upon activation triggers the activation of Arp2 and 3 which are directly implicated in actin polimeriìzation and actin dynamics (Campellone and Welch, 2010).

Additionally, CYFIP1 is also part of FMRP-eIF4E translational complex (Napoli et al., 2008). Since Cyfip1 engage between two complexes WRC and eIF4E, it has been shown that it could not be part of both of them simultaneously, thus is required a dissociation from one in order to be available to bind with the other complex. The data of crystallography has demonstrated that Cyfip1 when is engaged in WRC complex, at molecular level interacts extensively with NCKAP protein. In this binding site is also presented Lys743 which is essential for interaction with eIF4E (Napoli et al., 2008).

Furthermore, immunoprecipitation of eIF4E reveals the presence of CYFIP1 but not NCKAP, and similarly, immunoprecipitation of NCKAP shows the presence of CYFIP1 but not eIF4E, concluding that CYFIP1 participates in two distinct complexes. In this dual role of Cyfip1, Rac 1 plays a pivotal role on driving the presence of Cyfip1 either in WRC or eIF4E complex. Conformational changes of Cyfip1 from globular to planar could define its interaction between two distinct complexes. Indeed De Rubeis and colleagues have demonstrated that Rac1 promotes switch of CYFIP1 from globular to

planar conformation which lead to dissociation from eIF4E and binding with NCKAP leading through the formation of WRC complex.

Recent findings highlight the role of CYFIP1 in the NOTCH signaling pathway (Dziunycz et al., 2017; Habela et al., 2020). Given that NOTCH is crucial for maintaining the balance between symmetrical and asymmetrical division in neural stem cells (Egger, Gold and Brand, 2010; Contreras et al., 2018), CYFIP1 expression appears to be important in neural development processes.

3.3 The physiological role of CYFIP2

Cytoplasmic FMR1-interacting protein 2 (CYFIP2), also known as KIAA1168 or PIR121, is a protein-coding gene located on chromosome 5q33.3 (NC_000005.10). The CYFIP2 gene potentially encodes four isoforms, according to the UniProtKB Database (Q96F07). The primary protein product of CYFIP2 consists of 1,253 amino acids and is highly conserved, sharing 99% sequence identity with its mouse counterpart (Schenck et al., 2001). CYFIP2 is primarily expressed in brain tissues, white blood cells, and the kidney, as noted in studies by (Su et al., 2004). CYFIP2 is known as a binding partner of FMRP, and unlike CYFIP1, it also binds the paralogs FXR1P and FXR2P. The functional role of this interaction in biological processes is not yet fully established. De Rubeis and collaborators have shown that CYFIP2 binds FMRP and also the translation initiation factor eIF4E, which has been established as a binding partner of CYFIP1 as described above. Furthermore, CYFIP2 has been co-immunoprecipitated with eIF4E in rat primary cortical neurons (Tiwari et al., 2016). This interaction of CYFIP2, conserved at the C-terminus, has been investigated by Napoli and colleagues, suggesting a possible functional role of CYFIP2 in regulating FMRP-targeted mRNAs. Indeed, by sequestering eIF4E, CYFIP2 inhibits the scaffold protein eIF4G from binding eIF4E, which ultimately blocks cap-dependent translation (DeRubeis et al., 2013). It is plausible that the clustering of FMRP/CYFIP/WRC could regulate the translation of proteins involved in actin cytoskeleton dynamics, thereby impacting dendritic spine morphogenesis and other cellular functions.

So far, CYFIP2 has been extensively studied as a key member of the heteropentameric complex WRC. The most significant role attributed to it is in regulating actin dynamics. Indeed, through the

interaction of the VCA domain with Arp2/3 upon different upstream signaling, actin polymerization takes place, as described in more detail above. Recent studies have found that Cyfip2 interacts with 25 other proteins correlated with mRNA metabolism in mouse brains. Among all proteins studied Lee and collegoues found Pumilo 1 (PUM1) and Argonaute2 (AGO2) involved in mRNA processing and miRNA pathwayes, respectively.

Additionally, CYFIP2 has been found to be implicated in tumors. Indeed, circCyfip2, a splicing variant of the CYFIP2 transcript, has been described to act as a sponge for miR-1205, which regulates the expression of E2F1. This protein is upregulated in different forms of tumors. Li and colleagues suggest that the circCyfip2-miR-1205-E2F1 pathway is strongly involved in the migration and proliferation of gastric cancer, thus attributing to circCyfip2 a role as a biomarker of this disease (Lin et al., 2020).

CYFIP2 seems to have a larger implication in tumor pathogenesis. In 2007, Jackson and colleagues found a p53 responsive element in the CYFIP2 gene promoter. The p53 protein, encoded by the TP53 gene, is one of the most studied genes in cancer biology and is considered to be one of the most remarkable tumor suppressors. The responsive element in CYFIP2 leads to the activation of its transcription through the p53 factor. Considering this regulation at the transcriptional level, once p53 is lost in many forms of tumors, the expression levels of CYFIP2 could be altered (Ozaki and Nakagawara, 2011). Yet, more research is needed to establish the functional role of this crosstalk between CYFIP2 and p53.

Moreover, CYFIP2 is implicated in T cell adhesion. Indeed, Mayen and collaborators, by analyzing CD4+ cells in patients with multiple sclerosis, found increased levels of CYFIP2 expression. Since CYFIP2 is part of the WRC complex, its high level may promote T-cell adhesion. Healthy T cells with overexpression of CYFIP2 showed a higher level of adhesion compared to control. Also, CYFIP2 knockdown in CD4+ cells derived from patients showed lower adhesion (Mayne *et al.*, 2004). Still, the role of CYFIP2 in this cell population is not totally clear.

3.4 CYFIP2 and RNA editing

RNA editing is a posttranscriptional modification that refers to any RNA site specific substitution. It can be considered a mechanism that can increase biological information.

Two types of RNA editing are known to be present in mammalians and both implicate a deamination of a nucleotide in a double strand RNA. The output of this process is the conversion of Cytosine (C) in Uracile (U) or Adenosine (A) in Inosine (I).

In particular, A to I RNA editing is catalyzed by ADAR (Adenosine Deaminase Acting on RNA) enzymes, which by deaminating, convert the structure of a nucleotide leading to a new information. This conversation can have a multiple outcome and can modify the structure of protein or modifying splicing site and so on. Additionally, RNA editing can also affect RNA stability (Daniel, Behm and Öhman, 2015). So far, it has been well established that RNA editing that leads to deamination of adenosine to inosine, which can be readed as a guanosine by most of cellular machineries is a key mechanism to mark RNA as self. The other function attributed to A to I conversion as I mentioned before is recoding the information encoded in RNA, which ultimately leads to a new protein that differs in function and structure from its gnomically encoded version, amplifying thus the range of information.

Levanon and collaborators have revealed that CYFIP2 transcript can be edited by ADAR2 enzyme. The substitution A to I (resulting in a K320E substitution in protein) seems to be more present in brain cortex (Kwak, Nishimoto and Yamashita, 2008). Experiments in mice showed an increase of levels of editing of CYFIP2 in embryo stage reaching a peak in around 21 postnatal days. (Wahlstedt *et al.*, 2009). While another study showed a decrease of levels of editing in human brain over time. (Nicholas *et al.*, 2010). The editing of CYFIP2 doesn't change just over time but also is responsive to different conditions, for instance Bonini and collaborators have found that the edited form of CYFIP2 is decreased in primary cortical neurons treated with glutamate. This decrease has been attributed to decrease level of expression of ADAR2 which affects overall CYFIP2 editing. (Bonini *et al.*, 2015) These data taken together evidence the importance of editing during neurodevelopmental stages. Yet further research is required to establish this relationship between CYFIP2 and editing.

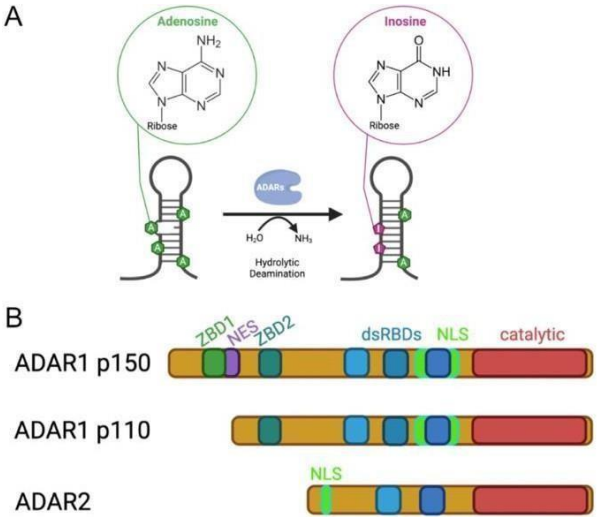

Figure 1.4: Illustration of RNA editing mediated by ADAR enzymes (Vesely and Jantsch, 2021)

3.5 CYFIP family member and neural disorders

Initially both, CYFIP1 and CYFIP2 have been identified as binding partners of FMRP protein whose absence leads to the Fragile X syndrome, suggesting a role of CYFIP1 and 2 in this form of neurodevelopmental disorder. Since then it has been reported an implication of CYFIP1 and CYFIP2 in a larger number of diseases, from neurologic disorders to lately even cancer. Indeed, both those two isoforms have a larger function in cell life jumping from actin dynamics to metabolism of RNA as described with more detail in the previous paragraph.

The first studies in vivo that indicate the importance of CYFIP protein in neuronal processes were conducted by Schenck in Drosophila. This species expresses just one homolog of CYFIP and dCYFIP mutant larva showed a reduction of length of synaptic terminal as well as an increased number of immature buds. The opposite phenotype was obtained in drosophila dFMRP (Pan et al., 2004). Indeed, it was observed that double homozygous mutant dFMPR and dCYFIP2 were comparable to WT. This data evidence a possible interaction between CYFIP and FMRP on regulating synaptic structure in Neuromuscular junctions (NJMs) in Drosophila.

Further, by investigating the localization of these two proteins Pathania and collaborators identified that both CYFIP1 and CYFIP2 are localized predominantly in dendritic spines specifically in excitatory postsynaptic mature neurons. Also, they reported that overexpression of either CYFIP1 or CYFIP2 leads to extended dendritic arborization in hippocampal neurons. A similar study was performed in vivo, CYFIP1 haploinsufficiency in mice but not CYFIP2 caused an increase in number in immature and long thin spines (Pathania et al., 2014). Also, Herman and colleague confirmed this data, indeed they found that overexpression of CYIFP1 overall increased spine frequency while haploinsufficiency caused an increase of immature spines and dysregulation of cytoskeleton in dendritic spines as Pathania reported (Pathania *et al.*, 2014). While mice with CYFIP2 haploinsufficiency displayed alterations in cortical dendritic spine maturation (Han et al., 2014). Also, CYFIP2 heterozygous mice exhibit abnormalities in the morphology of spines in adult CA1 pyramidal neurons. These data demonstrate that CYFIP1 and CYFIP2 are implicated in different neural disorders.

Another study in zebrafish evidence the role of both CYFIP1 and CYFIP2 in axonal cone growth. By integrating the molecular replacement strategy and time sequenced tracking of axon elongation they demonstrated an involvement of CYFIP2 in this process.

Particularly, in response to contact axon-axon CYFIP2 was translocated to the outgrowth cone to manage the filopodial dynamics thus to induce axonal sorting or repulsion. Deletion of CYFIP1 and CYFIP2with CRISPR-Cas9 caused impairment in axonal growth. This line of evidence suggested an implication of CYFIP1 in axonal growth and CYFIP2 in axonal sorting (Cioni et al., 2018)

Several studies have found implication of CYFIP1 and CYFIP2 in brain disorders but in clinically different types of brain diseases. Nevertheless, numerous studies in vivo and in vitro yet the exact role of CYFIP2 in neural function and dysfunction has been less well characterized compared to its homologues CYFIP1.

CYFIP1 has been linked with a large number of behavioral, cognitive, and neurodevelopmental disorders. Alteration of this protein has been found in autism spectrum disorders (Noroozi *et al.*, 2018), Intellectual disabilities (Clifton et al., 2020) and in schizophrenia (Domínguez-Iturza *et al.*, 2019). Patients affected by schizophrenia have reduced CYFIP1 mRNA levels in their peripheral blood, while those affected by epilepsy showed elevated levels (Sayad et al., 2018).

Moreover in different studies has been found an association of CYFIP1 with NLGN3 (Neurlignin 3). Interstingly in 2003 a correlation between ASD and NGL3 was described in two siblings (Jamain et al., 2003).

Further, Josef T Kittler and colleague have reported that CYFIP1 conditional knockout model upon neocortical cells leads to postsynaptic increase of expression levels of Neuolignin3 and $GABA_A$ B2/3 subunits, thus enhancing synaptic inhibition which has been associated with ASD. They also, demonstrated that Increased CYFIP1 levels selectively alter inhibitory and excitatory synapses. So far altered E/I balance has been considered hallmark for many neuropsychiatric and neurodevelopmental disorders. In addition to variation in terms of increase or decrease of CYFIP1 which have different consequences in different neural disorders, it has been identified that deletion or gains in chromosome 15q11-13 region where CYFIP1 gene locate is strongly linked with intellectual disabilities. (Butler, 2017). Patients with Behavior disorders and Prader Willi syndrome or Angelman Syndrome present deletion or duplication in specific loci. These loci, identified as breakpoints (BP1, BP2, and BP3), can undergo breaks occurring between BP1- BP2 (Burnside-Butler locus) BP1-BP3 (type I) or BP1-BP3 (type 2). Patients with more severe prognosis present breaks mostly in BP1-BP2 region. Another study conducted by Oguro- Ando and collaborators demonstrated that ASD patients carrying a duplication in the 15q11-13 region display higher expression levels of CYFIP1 in lymphoblastoid cell line and also in the temporal cortex. They also found that concomitantly with the increase of CYFIP1 there is an increase of mTOR levels and phosphorilation of S6 in the brain of these patient. This research suggest a role of CYFIP1 in the modulation of mTOR signaling linked with ASD (Oguro-Ando et al., 2015)

In line with this study also, CYFIP1 knockdown mice showed decreased of mTOR protein levels as well as phosporilaton S6 levels. Surprisingly cortical neurons isolated from Fmr1 knockout mice showed higher levels of S6 phosphorilation. Altered levels of CYFIP1 mRNA in terms of decrease has been reported also in the brain and lymphocytes of patient diagnosed with FXS, while the levels of two effectors of mTOR , S6K1 and AKT were interestingly increased (Abekhoukh et al., 2017).These reports suggest an important role of CYFIP1 on modulating mTOR signaling. This modulation may vary according to absence or presence of FMRP.

In line with other reports, deficits in dendritic spine shape and plasticity have been documented in the post-mortem tissue of people with various kinds of ASD, which is consistent with the fact that neuronal function is disrupted in ASD pointing CYFIP1 as the key disease-causing gene (Phillips and Pozzo-Miller, 2014).

Despite considerable knowledge about CYFIP1, the neuronal function and dysfunction of its paralog Cyfip2 are still largely unexplored. Although changes in CYFIP2 function have been linked to neurological and neuropsychiatric disorders via genetic correlations and alterations in expression; . Han et al., 2014. The first genetic findings linking CYFIP2to neuronal function in mice emerged from quantitative trait locus (QTL) analysis, which aimed to identify genetic loci responsible for the behavioral differences between the C57BL/6J and C57BL/6N mouse substrains. (Kumar *et al.*, 2013) (Kirkpatrick *et al.*, 2017). On the other hand a whole genome sequencing detected only 10000 single nucleotide polimorphisms (SNPs) between the substrains (Keane *et al.*, 2011) By taking advantage of QTL analysis, Kumar and collaborator revealed a SNP (G to A at the 46,036,117 base pair of chromosome 11). This SNP leads to a serine-to-phenylalanine missense mutation (S968F) in Cyfip2 gene which is responsible for a lower acute response and sensitization in mice under cocaine treatment. They also found a decrease spine density as well as a decrease frequency of mini-exitatory postsynaptic signaling currents mEPSC. Both of these characteristics are linked to drug-induced structural plasticity, and consequently, to addiction. (Kumar et al., 2013). Additionaly CYFIP2 S968F mutation has been found to be involved also in binge eating, obesity and overall eating disorders. Mice with this mutation exhibit compulsive eating behavior, potentially linked to the downregulation of myelination genes, which aligns with the observed reduction in white matter in patients with eating disorders.

CYFIP2 alteration has been associated also with cognitive defects, indeed Han and collaboratosr have observed that cyfip2+/- heterozygous mice show some fragile X syndrome behavior. In line with this study it has been found a reduction of CYFIP2 protein expression levels in FXS patient. (Hoeffer et al., 2012).

Moreover, CYFIP2 has been considered a possible candidate gene for the treatment of Alzheimer disease. Emerging research has found an increase of Aβ accumulation, memory deficits, synapse loss and gliosis in the brain of aged mice with CYFIP2$^{+/-}$ (Ghosh et al., 2020). Reduced expression levels of CYFIP2 have been associated with several changes, including hyperphosphorylation of tau protein, the formation of amyloid plaques, and ultimately, memory loss. (Tiwari *et al.*, 2016) Tau acts as microtubule-stabilizing and its phosphorilation leads to dislocation to dendritic spines with consequent deficits in microtubule integrity and organelle trafficking. This series of events may be the cause of the decrease in mitochondria numbers in the presynaptic region in the cortex of adult CYFIP2 heterozygous mice (Kim et al., 2020).

3.6 Discovery of *de novo* missense hotsposts in CYPIF2

Importantly, two recent studies have similarly detected de novo hotspot at Arg87 variants in the CYFIP2 gene in patients with Early Infantile Epileptic Encephalopathy (EIEE) (Nakashima *et al.*, 2018; Zhong *et al.*, 2019) The first study conducted by Nakashima and collaborators in 2018 documented for the first time a link between CYFIP2 and EIEE. In this study 489 patients with different forms of EIEE were recruited. They identified in four unrelated patients diagnosed with West syndrome three de novo CYFIP2 variants at the Arg87 residue (Arg87Leu, Arg87Cys, and Arg87Pro) (Fig 1.5). All four individuals experienced their first seizures before reaching the age of six months. Additional characteristic included hypotonia, microcephaly, developmental delay and intellectual disabilities. Also Peng and colleague by performing an WES analysis in 56 Chinese families with WEST syndrome found out 112 variants in 89 genes. Among all variants they identified again Arg87Cys of CYFIP2(Zhong *et al.*, 2019). Subsequent studies identified seven missense variants with p.Arg87Cys and p.Ile664Met occurring most frequently. (Zweier et al., 2019). Additionally, Begeman and collaborator in their studies identified other patients with the Arg87Cys variants and they also discovered new variants, Arg87His and Arg 87Ser. (Begemann et al., 2020)

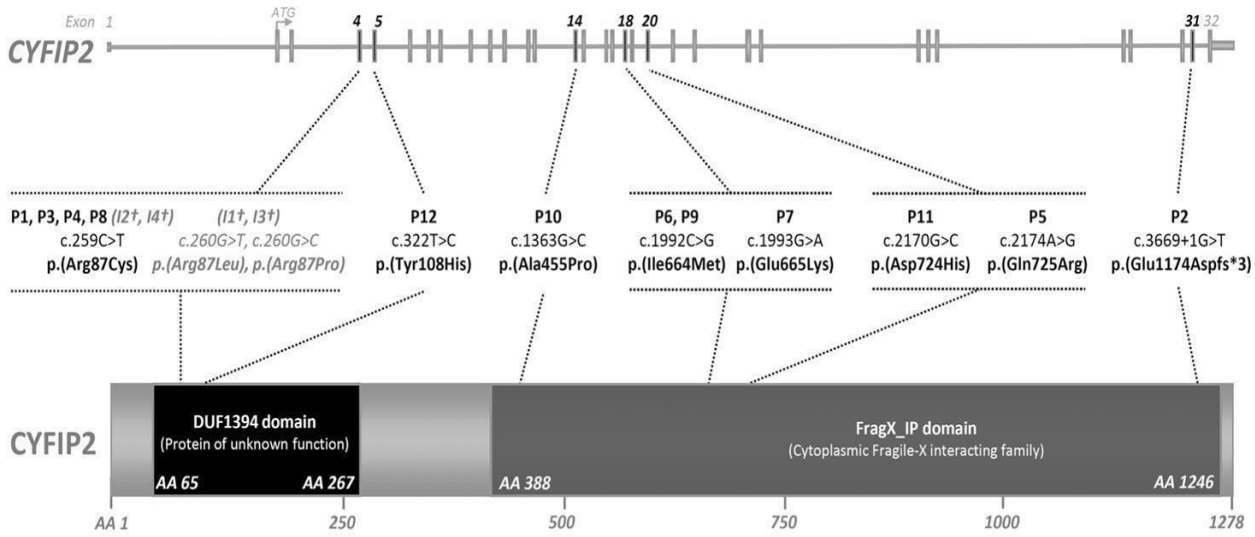

Figure 1.5: Schematic representation of CYFIP2 gene and localization in the exon 4 and 5 of R87 variants. Adapted by (Zweier *et al.*, 2019).

4.1 CYFIP2 R87C Variant and Early Infantile Epileptic Encephalopathy

Since Nakashima and colleagues discovered de novo hotspots of CYFIP2 at R87 residue (Fig 1.6) a lot of work has been done to assess their role in EIEE as well as in West Syndrome which is a specific subclasses of EIEE. Among all three variants at R87C documented by Nakashima, a growing amount of evidence suggest that R87C is the most common mutation and has the severest prognosis in patient with EIEE (Begemann et al., 2012 date; Zhong et al., 2019; Zweier et al., 2019). Even though the clear association between R87C and EIEE yet, the pathophysiological mechanism by which this mutation causes the disease is not fully assessed. After its discovery, Nakashima and collaborators tried to establish the impact of this mutation on WRC complex, since CYFIP2 is part of it. He took advantage of previously established crystal structure of WRC (Chen et al., 2010). Nakashima reported that R87 residue its positioned in the interface between CYFIP1 and WAVE1. It has been studied on CYFIP1 because the solved structure of WRC contains CYFIP1 instead of CYFIP2. He found out that R87C interact with both WAVE 1 and CYFIP1 by creating a hydrogen bound with the main chain Tyr151 and the side chains of Glu625 and Glu690 respectively. Especially this study suggested that all of three variants of R87C were predicted to interrupt the hydrogen bonds between CYFIP1 and WAVE1.

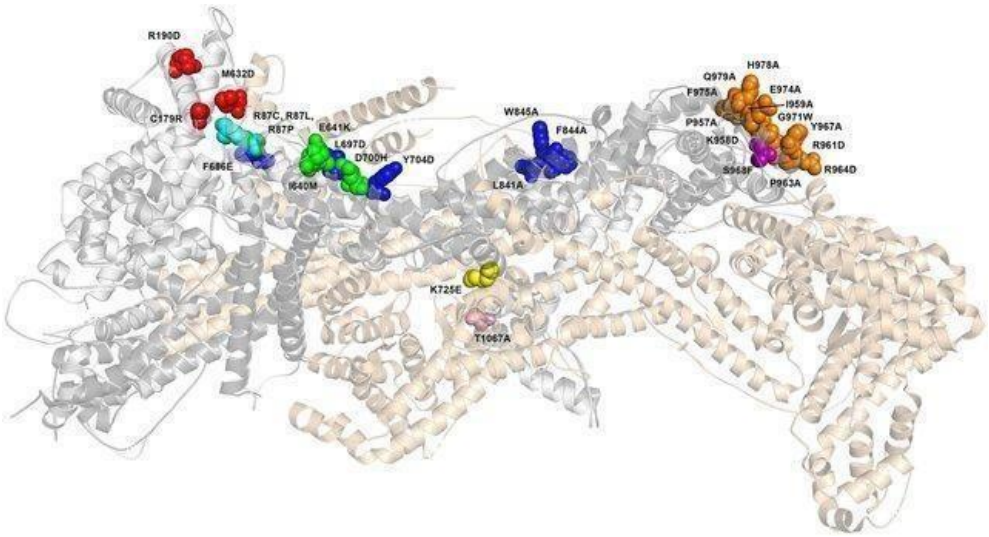

Figure 1.6: A model of the CYFIP1/2 protein (depicted in dark grey/light grey) interacting within the WRC complex (shown in wheat). The CYFIP2 model was generated using Modeller, with the CYFIP1 structure serving as the template (PDB: 3P8C, given that CYFIP1 shares 95% similarity with CYFIP2). The other WRC chains were derived from the PDB structure 3P8C. Spheres highlight regions where mutations in CYFIP proteins have been linked to biological effects. Mutations

identified in CYFIP2 include R87C, R87P, and R87L, which are associated with a weaker interaction between CYFIP and the VCA domain of WAVE (cyan). The S968F mutation is associated with protein destabilization (purple), while the T1067A mutation is linked to reduced density of stubby spines in cultured hippocampal neurons (pink).(Adapted from (Biembengut et al., 2021)

The weak interaction of CYFIP2 within the WRC complex has been hypothesized as key mechanism of pathophysiology of R87C in EIEE (Biembengut et al., 2022). Indeed, Nakashima and collaborators has revealed that all three variants have a lower interaction with purified VCA domain of WAVE compared to WT CYFIP2 (Nakashima et al., 2018). Moreover, they observed an abnormal increase of F-actin accumulation in cultured mouse melanoma cells transfected with CYFIP2 mutant compared to WT (Nakashima et al., 2018). This theory was supported also by Schaks and colleagues, they observed a recovery of lamellopodia formation by inducing expression of Arg87Cys in CYFIP1-2 KO cells and the same phenotype is observed also by inducing VCA domain. Additionally, the recovery of lamellopodia formation induced by R87C is observed even in absence of Rac1 which is a key component to trigger this signaling. These data suggest a constant activation of WRC complex in presence of CYFIP2 mutation even in absence of stimuli (Schenck et al., 2001). Further, other studies have attributed to R87C a role in the formation of stress granule (SG). Lee and collaborator observed differences in stress granule formation in HeLa cells by overexpresseing (EGFP) CYFIP2 WT or variants of CYFIP2 (R87C, R87L, R87P, I639M or E640K). Then they co-stained with Ras-GTPase thus, activating (G3BP) which is used as marker for SG. This experiment was performed under basal conditions and oxidative stress induced by using sodium arsenite ($NaASO_2$). (Lee et al., 2020).They observed that only three R87 variants of CYFIP2 formed intracellular clusters despite the presence or absence of $NaASO_2$ treatment. This effect was not observed neither in CYFIP2 WT and other two variants I639M or E640K. While under basal condition in Hela cells overexpressing CYFIP2 WT or variants I639M or E640K SGs were not formed. The opposite effect was obtained under $NaASO_2$ treatment with presence of SGs in almost 90% of cells. Interestingly this result was not the same for the three variants of R87. Indeed the presence of SGs was observed only in 49-72% of the cells suggesting a role of R87 variants in SGs formation. Moreover, even in cells where R87 variants were overexpressed and stress-induced SGs formed, these SGs did not overlap with CYFIP clusters; instead, they appeared to be distinct from each other.
Accordingly, Lee and colleague hypothesized that probably CYFIP2 R87 could potentially include intrinsically SG, thus preventing the successful assembly of SGs as it was observed in WT and other varaints not at R87 residue (Lee et al., 2020).

By using computational modelling it has been assesed that low interaction of CYFIP2 R87 with WAVE and consequently costant activation WRC is the main mechanism of pathogenicity of variants at 87 residue. Beyond this hypothesis, it has been suggested that R87 variants could affect RNA binding protein RBP- associated with CYIFP functions including mRNA- silencing or SG formation. This alteration may be caused due to induced formation of intracellular CYFIP2 clusters. Even though is yet far from clear the exact mechanism by which R87 variants induce CYFIP2 clusters. However the accumulation of this clusters may activate proteostasis system to clear it up resulting though in overall reduced levels of CYFIP2 protein. (Zhang, Lee and Han, 2019).

By generating a heterozygous mice carrying the R87C variant Han and colleague found a reduced level of CYFIP2 in mutant mice compared to WT. Regarding the neurobehaviour pattern they also observed differences between CYFIP2 heterozygous and CYFIP2$^{+/R87C}$. Specifically, CYFIP2$^{+/R87C}$ mice showed increased hyperactivity, reduced anxiety and enhanced seizure susceptibility compared CYFIP2 heterozygous. Interestingly it was observed an increase of F- actin accumulation specifically in mPFC of CYFIP2$^{+/R87C}$ and not in the other brain regions. This increase of F-actin could be due to the low interaction of CYFIP2 R87 with WAVE leading to aberrant activation of WRC as widely described by many authors. The reason why this decrease occurs only in mPFC, the authors Han and collaborator suggest that may be because of lack of compensation by its paralog CYFIP1 since is not expressed in mPFC.

4.2 Overview, Developmental and epileptic encephalopathies DEEs.

Developmental and epileptic encephalopathies DEEs are a group of severe neurological disorders with onset in infancy or early childhood. The term developmental was introduced because of various factors that lead to developmental impairment in affected individuals. They are characterized by frequent refractory seizures and are considered clinically and genetically heterogeneous. Both, seizures, and underlying conditions of etiopathology lead to severe neurodevelopment dysfunction. DEEs are classified in: Ohtahara syndrome, Early myoclonic encephalopathy, Epilepsy of infancy with

migrating focal seizures, all of them have early onset usually within three months of life and in same case even the first two weeks of life.

WEST syndrome, Dravet syndrome, Myclonic atonic epilepsy have an infantile onset starting from three months to two years of life. The third subset of DEEs are: Rasmussen Syndrome, Lennox Gastaut syndrome and Epilepsy-aphasia spectrum: LKS/CSWS, which are characterized by late onset usually in childhood after the second years of life.

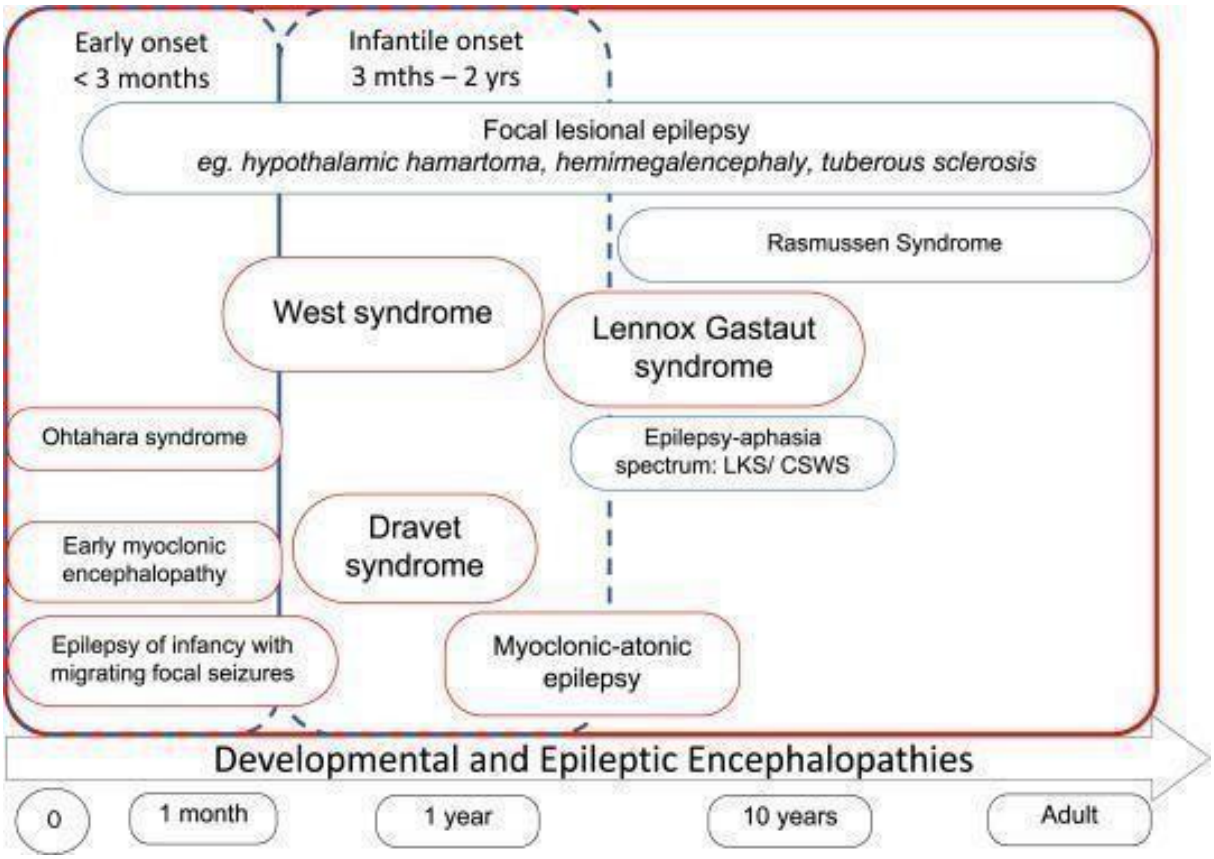

Figure 1.7: Schematic representation of Developmental and Epileptic Encephalopathies, adapted from (Scheffer *et al.*, 2017)

4.3 Early infantile epileptic encephalopathy EIEE

Early Infantile Epileptic Encephalopathy (EIEE) is a subclass of DEEs (Auvin, Cilio and Vezzani, 2016) also known as Ohatahara syndrome (Ohtahara et al., 1987).EIEE is a severe form of epilepsy that typically manifests within the first few months of life, usually before the age of three months and in some cases even in the first weeks of birth (Kato et al., 2004).EIEE are characterized by burst-suppression pattern on electroencephalogram often leading to early death (Radaelli et al., 2018), frequent and severe seizures, developmental delay or regression, and abnormal brain function. EIEE represents a severe form of epilepsy with a poor prognosis. Infants suffering from EIEE often experience frequent and refractory seizures, which can take the form of tonic, myoclonic, suckling reflexes, hypotonia of the muscles (Cheng et al., 2017). The occurrence of these symptoms is not affected by circadian rhythm, thus wake up or sleeping time, indeed patient may exhibit symptoms even hundreds of times in 24 hours. Additional seizure types that patients might face consists in ~~in~~ hemic seizures, focal motor seizures (Malik et al., 2013). These seizures typically begin in the first few months of life and standard anti-epileptic treatment involves drugs such as levetiracetam, valproate, phenobarbital, zonisamide and benzodiazepines. In some cases, a ketogenic diet has been shown to be effective in reducing the frequencies of seizures as well as to induce a better response to anti-epileptic drugs. Additionally, another form of therapy in some patients consist in chirurgical removal of brain areas indicated as responsible for the generation of seizures, which in many cases lead to considerable improvement. Unfortunately, some patient does not respond to pharmacological therapy making very challenging symptoms attenuation. The relentless seizures lead to development stagnation and, in some cases severe intellectual disabilities. Seventy-five percent of EIEE patient turn in WEST syndrome within 3 to 6 months which has an incidence 0,16-0,42 in thousand births (Ducal O et al.,2001). In this case seizures manifest I various forms and typically occur suddenly and usually are bilateral and symmetrical which may involve flexor, extensor or a combination of both types, impacting thus the neck, body and extremities (Hancock, Osborne and Edwards, 2013). Another percentage of patient shifted in WEST Syndrome turns into Lennox -Gastout syndrome which is rare form of epileptic encephalopathy (Jain, Sharma and Tripathi, 2013). LGS has the onset between 1-8 years with a peak around 3-4 years. Seizures are etiologically regrouped into symptomatic and cryptogenic types. The majority fall under cryptogenic, whereas sympotomatic seizures are secondary to underlying pathologies such as

hypoxicischemic encephalopathy, Down's syndrome, brain tumor, vascular damage, and perinatal meningoencephalitis. (A.Beaumanoir et al.,2002) In LGS, 74%-90% of seizures fall into tonic seizures and the second most common symptoms are atypical absences.

4.4 Genetic underpinning EIEE.

The genetic underpinnings of EIEE have gained increasing attention due to their role in the development and progression of this condition as well in diagnosis. The incidence of this age-related disorder has been estimated between 1:50000 and 1:100000. (Poke et al., 2023). Thus far, by using genetic techniques such as whole genome analyses and NGS has been revealed a link between EIEE and more than 50 distinct disease-causing genes. (Ostrander et al., 2018). Among all the genes that that has been identified to contribute to the pathophysiology of these group of disorders, CYFIP2 mutation has been identified as a genetic contributor to EIEE. So far, 20 deleterious has been identified and in 2018 Nakashima and other researchers identified three mutational de novo hotspot at codon 87 of CYFIP2, associated with particularly a severe form of EIEE. The prevalence of de novo mutations of CYFIP2 in EIEE is yet not reported. In literature so far is reported that infants carrying these de novo mutation has grim prognosis and severe development delays.

Moreover, they also showed a resistance to classical antiepileptic pharmacological treatment leading the whole thing more difficult. (Da Silva Cardoso et al., 2023)

Despite the progress to date the mechanism by which CYFIP2 mutations lead to EIEE is still under investigation but is believed that the disruption of synaptic signalling and neural plasticity caused by the mutation may contribute to the epileptic encephalopathy.

Further, diagnosis of these severe pathologies continuous to be difficult for physician since there is not a standardized clinical protocol. In this long excursus among the other clinical tests, such as radiological imaging or metabolic testing, the generation sequencing has played a pivotal role in revealing the monogenic causes. Even though the wide use of genetic approaches over years, yet the success rate of diagnosis by using gene panel or whole genome sequencing is yet under 60% making the diagnosis very challenging as well as treatment.

2. AIM

Cytoplasmic FMRP Interacting Protein 2 (CYFIP2) is a pivotal regulator of actin dynamics, which underpin essential cellular processes such as cell division, migration, and the development of specialized neuronal structures like dendritic spines and axonal growth cones. These processes are crucial for synaptic plasticity and the maintenance of neural circuits. Disruptions in CYFIP2 function are strongly linked to neurodevelopmental disorders, highlighting its critical role in neural physiology.

In 2018, Nakashima and colleagues identified three de novo mutations in the *CYFIP2* gene, R87C, R87L, and R87P associated with severe neurodevelopmental conditions, including Early-Onset Infantile Encephalopathies and West Syndrome. Among these mutations, R87C emerged as the most frequently observed variant and was associated with the poorest clinical outcomes.

This thesis focuses on understanding the role of CYFIP2 in neuronal development and exploring the pathological effects of the R87C mutation. Using in vitro models, including a neuroblastoma cell line and primary hippocampal neurons, a range of morphological and functional parameters were analyzed to characterize the mutation's impact. These findings aim to shed light on the underlying mechanisms of R87C-related pathologies and contribute to potential therapeutic insights.

3. MATERIAL AND METHODS

1.1 Cell culture

1.1.1 HEK293T

Cells were plated at 37°C and 5% CO2 in DMEM medium (Invitrogen) supplemented with 10% of heat-inactivated fetal bovine serum (FBS), 30 U/mL Penicillin, 30 mg/mL Streptomycin (Sigma-Aldrich®), 1% minimum Eagle's medium nonessential amino acids (GibcoTM, Thermo Fisher Scientific), 1 mM sodium pyruvate (GibcoTM, Thermo Fisher Scientific). Cells were split at approximately 80% confluency.

1.1.2 SH-SY5Y Neuroblastoma cell line

The human neuroblastoma SH-SY5Y cell line was purchased from the American Tissue Culture Collection (ATCCTM, CRL2266). SH-SY5Y CYFIP2-KO was generated in our laboratory taking advantage of CRISPR-Cas9 technology. Both cell lines have been grown in 1:1 mixture of Ham's F12 Nutrient Mix (#11765054 GibcoTM, Thermo Fisher Scientific) and Dulbecco's modified Eagle's medium, (DMEM, #D6429, Sigma-Aldrich®) containing high glucose (4500 mg/L), L-glutamine (4 mM) and sodium pyruvate (1 mM). This medium was supplemented with 10% (v/v) heat-inactivated fetal bovine serum (FBS, #10270, GibcoTM) and 1% antibiotic antimycotic solution (#A5955, Sigma-Aldrich®). Cells will be cultivated in T175 flasks at 37 °C with 5% CO2 at saturated humidity and kept below ATCC passage + 15 to avoid cell senescence.

1.1.3 SH-SY5Y Neuroblastoma cell line differentiation

To differentiate SH-SY5Y cells, we employed a well-established method that uses a combination of retinoic acid (RA) and brain-derived neurotrophic factor (BDNF), following the protocol described by Hromadkova et al. (2020). Initially, SH-SY5Y cells are seeded at a density of 1×1041 \times 10^41×104 cells/cm² on poly-D-lysine pre-coated 8-well slides, specifically prepared for confocal microscopy. On day 0, the cells are seeded and grown in a medium known as RALS, which is composed of DMEM/F12 in a 1:1 ratio, 3% fetal bovine serum (FBS), Penicillin/Streptomycin (P/S), 4 mM L-glutamine, and 10 µM RA. The medium is refreshed every 48 hours to ensure optimal growth conditions. After the initial growth phase, the culture medium is replaced with RANBB medium to induce differentiation. This new medium consists of NeuroBasal medium, B27 supplement, Penicillin/Streptomycin (P/S), 4 mM L-glutamine, 10 µM RA, and 50 ng/ml BDNF. The medium in this phase is changed every two days. By following this regimen, the cells undergo differentiation and are then considered ready for further experimental use.

1.1.4 Primary Hippocampal neuron culture

Primary hippocampal neurons were prepared as described in Goslin and Banker, (Schacher, 1992). Briefly, mouse hippocampi from embryonic day 16.5 were dissociated mechanically and neurons were resuspended in NeurobasalTM medium supplemented with B27 (GibcoTM, Thermo Fisher Scientific) containing 30 U/ml Penicillin, 30 mg/mL Streptomycin (Sigma-Aldrich®), 0.75 mM Glutamax (GibcoTM, Thermo Fisher Scientific) and 0.75 mM L-Glutamine (GibcoTM, Thermo Fisher Scientific). Depending on following experiments, neurons were seeded 100.000 cells/ 2 cm2 on 0.1 mg/mL Poly-D-Lysine-coated glass coverslip or 250.000 cells/ 10 cm2 in 0.02 mg/ml Poly-D-Lysine-coated 6- multiwell plates and maintained at 37°C under a 5% CO2 humid atmosphere. Three days after seeding, half of the medium was replaced with 24 hours-astrocyte- conditioned medium. After, half of the medium was changed every seven days up to a maximum of four weeks. Primary hippocampal neurons were prepared as outlined by Goslin and Banker, as referenced in Schacher (1992). The process began with the mechanical dissociation of hippocampi from embryos at day 16.5. The dissociated neurons were then resuspended in Neurobasal™ medium supplemented with B27 (Gibco™, Thermo Fisher Scientific). This medium included 30 U/ml Penicillin, 30 mg/mL Streptomycin (Sigma-Aldrich®), 0.75 mM Glutamax (Gibco™, Thermo Fisher Scientific), and 0.75 mM L-Glutamine (Gibco™, Thermo Fisher Scientific) to support neuronal health and growth. Depending

on the specific experimental needs, neurons were seeded at densities of either 100,000 cells per 2 cm^2 on 0.1 mg/mL Poly-D-Lysine-coated glass coverslips or 250,000 cells per 10 cm^2 in 0.02 mg/mL Poly-D-Lysine-coated 6-multiwell plates. These cultures were maintained in a controlled environment at 37°C with a 5% CO2 humid atmosphere, ensuring optimal conditions for neuronal survival and differentiation. Three days after the initial seeding, the medium was partially replaced: half of it was substituted with 24-hour astrocyte-conditioned medium. This step is critical as the conditioned medium provides essential factors that promote neuronal maturation and synaptic development. Following this initial medium change, the cultures were maintained with regular medium changes. Specifically, half of the medium was replaced every seven days, which helps maintain the nutrient balance and remove waste products, ensuring the cells remain healthy and viable. This routine was continued for up to four weeks, allowing sufficient time for the neurons to differentiate and establish mature networks.

1.2 Molecular biology techniques

1.2.1 Total RNA Isolation

Neuronal cultures at different DIV or cell cultures growing in adhesion were washed with RNAse-Free PBS and mechanically harvested in 1 mL of TRIzolTM (Thermo Fisher Scientific). An equal amount of 100% ethanol was added to each sample lysed in TRIzolTM and mixed thoroughly. The mix was transferred into a *Zymo-SpinTM* Column and centrifuged at 12,000 g for 30" to ensure RNA binding to the column. The column was then incubated with 80 µL of DNase I 15' at RT for digesting DNA. After two washes with *Direct-zolTM RNA* PreWash (12,000 g for 30'') and one wash with *RNA Wash Buffer* (12,000 g for 30''), the RNA bound to the column was eluted with 40 µL of Dnase/Rnase-Free water. The concentration of the eluted RNA was measured on a NanodropTM ND-1000 Spectrophotometer (Thermo Fisher Scientific).

1.2.2 Reverse transcription

Total RNA was reverse transcribed using Moloney Murine Leukaemia Virus Reverse Transcriptase (M-MLV RT) (ThermoFisher Scientific). 1 µg of each template RNA was incubated with 0,3 µg/mL Random Primers (ThermoFisher Scientific), 10 mM dNTPs (ThermoFisher Scientific), 5X First Strand Buffer (250 mM Tris-HCl (pH 8.3), 375 mM KCl, 15 mM Magnesium Chloride; ThermoFisher Scientific), 0,1 M DTT (ThermoFisher Scientific), 200U M-MLV RT (ThermoFisher Scientific), and water to a final volume of 20 µL at 37°C for 2 h followed by 10 minutes at 75°C to inactivate the enzyme.

1.2.3 cDNA amplification

To perform PCR reactions of the target genes, normalised amounts of the RT products was mixed with 12.5 µl of 2X DreamTaqTM Green PCR Master Mix (Thermo ScientificTM) and 1 µl of each forward and reverse primer (25 pmol/µl), to a final volume of 25 µl. PCR reaction was performed using the recommended thermal cycling conditions outlined below: one denaturation step for 2 min at 95 °C, followed by the appropriate number of cycles with 30 s of denaturation at 95 °C, 20 s of primer annealing at 60 °C, 30 s of elongation at 72 °C following by a final extension of 1 min.The primers used to amplify the cDNA sequence subjected to the RNA editing process are listed in Table

hCYFIP2 EF	GCCAAGAAGAGAATTAATCTTAGCAAAATTG
hCYFIP2 ER	ACTGGGGGCTGATGCTGCTCTG

Table 1: List of primers used to amplify the cDNA sequence subjected to the RNA editing process.

1.2.4 Sanger sequencing

The PCR reactions were purified through ExoSAP® according to the manufacturer's instructions. Briefly, 5µl of PCR were incubated with 1.5µl of ExoSAP mixture (1:2 ratio of exonuclease and shrimp alkaline phosphatase, SAP) for 15 min at 37°C and then the enzymes were inactivated for 15' min at 85°C. After PCR purification, the Sanger sequencing reaction were performed using Mastercycler Gradient (Eppendorf S.r.l.). The reaction mix is composed of: 1µl of terminator ready reaction mix;

1.5µl of dilution buffer, 1µl of 4 pmol/µl primer, 20ng of purified PCR and water until the final volume of 10µl is reached. The extension program is designed like this: 1 min at 95°C, followed by 25 cycles of repeated three steps made of 10 sec at 96°C, 5 sec at 55°C, 4 min at 60°C. After this process, another purification step is made with Performa® Dye Terminator removal (Edge BioSystems) columns to eliminate all the excess of fluorescent terminator dye. Then, the samples are dried at 95°C, resuspended in formamide and denatured at 95°C for 3 min before being processed through SeqStudioTM Flex Genetic Analyzer (ThermoFisher Scientific). The primers used to sequencing the vector pRRLSIN.cPPT.PGK-hCYFIP2-HA.WPRE are displayed in table 2.

hCYFIP2 352 For	GAGGTCACCAAGCTCATGAAGTTCATG
hCYFIP2 427 Rev	GCCGCTTCACCTCGCTGCAGAA
hCYFIP2 1366 For	ATGATCAAAGGCCTGCAGGTGCTC
hCYFIP2 2331 For	ATCCTTGGACCAAGCTATCAGCCG
hCYFIP2 2891 For	ATGAGTATGGCTCCCCAGGGATC
hCYFIP2 3370 For	GTGGAGTTCCACCGGCTGTGGA
hCYFIP2-436 Rev	AAAGTCCTTCCTGCGCTCGG
hCYFIP2-1450 Rev	GTCACCTGGGCGAAGTCCT
hCYFIP2-2327 For	TAAATCCTTGGACCAAGCTATCAG
hCYFIP2-2853 For	ATAGAGGTGATGCCCAAGATATGC
hCYFIP2-3516 For	TTTGACCTGTTCGACTTCTGTTACCA

Table 2: List of primers used to sequence the vector pRRLSIN.cPPT.PGK-hCYFIP2-HA.WPRE.

3.1 Cloning of human *CYFIP2* coding sequence

After total RNA purification from murine cortical tissue using RNeasy mini-kit (QuiagenTM), we perform a retrotranscription reaction (M-MLV Reverse Transcriptase, InvitrogenTM). cDNA generated is used to amplify *CYFIP2* whole CDS through PCR reaction with Q5 High-Fidelity® DNA polymerase (New England BiolabsTM) using a couple of primer shown in the Table 3.

hCYFIP2_AgeI_ATG_For	TTACCGGTCGCCACCATGACCACGCACGTCACCCTG
hCYFIP2_HA_TAA_SalI_Rev	ATTGTCGACTTAAGCGTAATCTGGAACATCGTATGGGTAGCAAGTGGTGGCCAAGG

Table 3: List of primers used to amplify the full length CDS of human CYFIP2 transcript.

Primers contain respectively AgeI and SalI restriction site, which will use to insert the amplicon in to pRRLSIN.cPPT.PGK-GFP.WPRE Lentiviral vector (#12252 AddgeneTM - Trono Lab). Reverse primers also contain sequence coding HA-TAG.
The enzymatic digestion of 1µg of CYFIP2 PCR product and pRRLSIN.cPPT.PGK-GFP.WPRE plasmid was carried out through SalI FastD 10 U/µl (Thermo Fisher Scientific) and AgeI 10 U/µl (Thermo Fisher Scientific) in Buffer Orange (Thermo Fisher Scientific) for 3h at 37°C. The subsequent inactivation was accomplished for 10' at 65°C. Then 20µl of digestion product were dephosphorylated with the Shrimp Alkaline Phosphatase (SAP InvitrogenTM) 30' at 37°C, followed by the enzyme inactivation 10' at 65°C. After the purification and gel quantification of the digestion products, the ligation reaction was set up in a volume of 20µl with a ratio 1:3 of empty vector (50ng) and *CYFIP2* insert DNA respectively, 1µl T4 DNA Ligase 5U/µl (Thermo Fisher Scientific) and T4 DNA Ligase Buffer 10×; the reaction mixture was maintained 1h at 22°C. Once obtained the ligation product, pRRLSIN.cPPT.PGK-hCYFIP2-HA.WPRE, the bacterial transformation was carried out using TOP10 bacteria strain (Thermo Fisher Scientific). After an overnight growth at 37°C on a LB-Agar plate under Carbenicillin selection, one CYFIP2 positive colony was selected for a subsequent MIDI-Prep preparation (MNTM kit) according to the manufacturer instructions. We perform a Sanger sequencing of plasmid DNA to confirm the absence of mutations within the generated sequence.

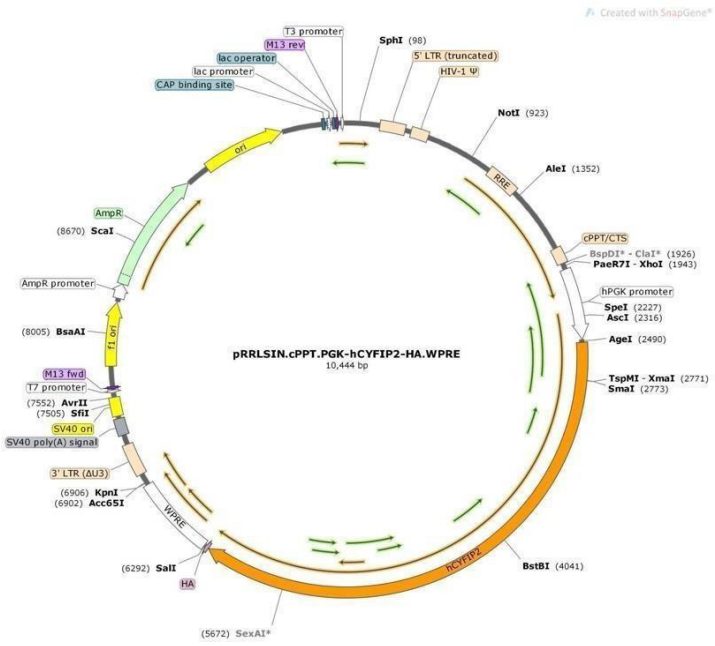

Figure 3.1: Lentiviral vector pRRLSIN.cPPT.PGK-hCYFIP2-HA.WPRE generated from pRRLSIN.cPPT.PGK-GFP.WPRE plasmid backbone (#12252 AddgeneTM - Trono Lab). The insert consisting of the CDS of human CYFIP2 transcript (NM_001037333.3) is orange-highlighted.

4.1 In vitro mutagenesis

To generate R87C mutation form of the lentiviral CYFIP2 vector, we start with in vitro mutagenesis. This involves introducing point mutations into plasmids using primers designed with the desired mutation. These primers are used in a PCR protocol that amplifies the entire plasmid template. Initially, the primers are carefully designed to incorporate the specific mutation into the CYFIP2 gene.

Figure 3.2: Schematic representation of in vitro mutagenesis.

After designing and synthesizing the primers, the plasmid DNA template is amplified using the Phusion™ Site-Directed Mutagenesis Kit from Thermo Fisher. This process uses Phusion™ Hot Start II DNA Polymerase along with the primers. The PCR protocol consists of 15 cycles, each involving denaturation at 98°C for 8 seconds and an extension at 72°C for 4 minutes. After the PCR amplification, the original parent template is removed by digestion with the methylation-dependent endonuclease DpnI, also from Thermo Fisher. The digestion takes place at 37°C for 1 hour and 30 minutes, ensuring that only the newly synthesized DNA, which incorporates the desired mutations, remains intact.

hCYFIP2-Mut-R87C For: TCATGCTGTACACCTGGTGCAGCTGTTCCCG
hCYFIP2-Mut-R87C Rev: CGGGAACAGCTGCACCAGGTGTACAGCATGA

Table 4: List of primers used to amplify the cDNA sequence subjected to point specific mutagenesis.

Following the digestion, the bacteria are transformed with the DpnI-treated, nicked plasmid. Once the transformation is complete, plasmids are isolated from the resulting bacterial colonies. These plasmids are then screened to identify those that contain the desired mutation. To ensure accuracy, the positive clones undergo sequencing. This step confirms the presence of the desired mutation and checks for the absence of any additional, unintended modifications.

4.2 Calcium Phosphate Transfection

The Calcium Phosphate Transfection method is a widely used technique for introducing DNA into cells. This method relies on the formation of a calcium phosphate-DNA precipitate. The precipitate facilitates the binding of the DNA to the cell surface, allowing the DNA to be taken up by the cells through the process of endocytosis.

4.3 Anysomycin treatment

HEK293T cells have been treated with anisomycin 40 µM at different time point 4h, 8h. Anisomycin is a bacterial antibiotic, potent inhibitor of protein synthesis. It disrupts both protein and DNA synthesis by targeting peptidyl transferase, an essential enzyme in the 80S ribosome system, thereby hindering the translation process. This molecule is used to block translation to evolute subsequently the degradation protein speed rate. After each time point the cells were harvested in RIPA buffer to proceed subsequently with protein extraction and then western blotting.

4.4 Protein extraction and quantification

Cells collected were solubilized using a modified RIPA buffer. This buffer comprised 50 mM Tris-HCl (pH 7.4), 150 mM NaCl, 1 mM EDTA, 1% IGEPAL CA630, 0.25% sodium deoxycholate, 0.1% SDS, 1% NP-40, and Roche protease inhibitor tablets. Following solubilization, the cells were sonicated applying 10 amper for 30 second to lysate totally the cells realizing so the protein in solution. A portion of the lysate was then used for the bicinchoninic acid (BCA) protein concentration assay (Sigma-Aldrich®).

4.5 Western Blotting

Equal amounts of protein were loaded onto homemade SDS polyacrylamide gels (4–12% NuPAGE Bis-Tris gels) and electrophoretically transferred applying 300mA to a nitrocellulose membrane (GE Healthcare, Waukesha, WI, USA) for 2 hours. The membranes were then blocked for 60 minutes with 3% non-fat dry milk in TBS-T (Tris-buffered saline with 0.1% Tween-20, Sigma-Aldrich®) and incubated overnight at 4°C in the blocking solution containing rabbit polyclonal anti-CYFIP2 (1:1000; #ab95969 Abcam, Cambridge, GB) and mouse monoclonal anti-GAPDH (1:10000, #MAB374 Millipore, Billerica, MA) primary antibodies. For protein detection, after at least three washes in TBS-T, the membranes were incubated for 1 hour at room temperature with IR-Dye secondary antibodies (1:2000 in TBS-T). Signals were detected using an Odyssey infrared imaging system (LI-

COR Biosciences) and quantified using Odyssey version 1.1 (LI-COR Biosciences). Data are presented as the ratio of the intensity of the band of the investigated protein to that of the GAPDH band and are expressed as a percentage of the controls. Each condition was performed and analyzed in three independent primary culture dishes.

4.6 Immunofluorescence assay

The cells were fixed paraformaldehyde (PFA) 4% then washed three times with phosphate buffer saline (PBS) and permeabilized with Triton-X-100 0,3% for 10 minutes at room temperature (RT). After the saturation with blocking solution for 1 hour at RT the cells were incubated with primary antibody. After three washes with PBS the cells were incubated with secondary antibody for 1h at RT. The cells were washed again for three times with PBS and then the DAPI staining was performed. The coverslips were then mounted SlowFade Gold reagent and observed under fluorescent microscope.

4.7 Lentivirus production

HEK293T cells are utilized for lentivirus production and are plated at low passages, specifically no more than P12-15. The cells are seeded 24 hours before transfection at a density of 9.5×10^6 cells in a 150 mm dish, with the medium being replaced 2 hours before transfection. The cells are co-transfected using the calcium-phosphate–DNA co-precipitate method. For the transfection, a mix of third-generation transfer plasmids is used, incorporating a hybrid LTR promoter. This plasmid mix is prepared by combining 7 µg of the VSV-G envelope gene in the pMD2.G backbone vector, 16.25 µg of the packaging plasmid pCMV ΔR8.74 II Gen.Pack, 6.25 µg of the pRSV-rev plasmid, and 32 µg of the transfer vector containing the CYFIP2-WT/Arg87Cys transgene. The plasmid solution is brought to a final volume of 1225 µl with 0.1× Tris-EDTA (TE 0.1×) and deionized water in a 2:1 ratio. Finally, 125 µl of 2.5M $CaCl_2$ is added to the suspension, which is then maintained at room temperature for 5 minutes. The precipitate is formed by adding 1250 µl of 2× HBS solution dropwise to the mixture, which should then be added immediately to the cells. The calcium-phosphate plasmid DNA mixture

is allowed to incubate with the cells for 14 to 16 hours, after which the medium is replaced with fresh medium. Cell supernatant is collected at 24 and 48 hours after the medium replacement. This supernatant undergoes ultracentrifugation at 23,000 rpm for 2 hours at 4°C. The resulting viral pellet is then resuspended in 1× PBS, ready for further use.

5.1 Generation of SH-SY5Y KO by using CRISPER CAS 9 technology

The CRISPR/Cas system can be effectively utilized in mammalian cells by co-expressing the S. pyogenes Cas9 (SpCas9) nuclease along with guide RNA. We employed this technology to establish an SH-SY5Y knockout (KO) cell line deficient in both CYFIP2 alleles (CYFIP2−/−). The SH-SY5Y CYFIP2 KO cell line was generated by transfecting wild-type (WT) cells with the plasmid px459 (SpCas9(BB)-2A-Puro (PX459) V2.0), created by Feng Zhang (Ran et al., 2013). This plasmid contains two expression cassettes: a human codon-optimized SpCas9 and a single guide RNA (sgRNA). The sgRNA includes a 76-nucleotide scaffold required for Cas9 binding and a 20-nucleotide spacer that targets the genomic sequence to be edited. The sgRNA is expressed under the control of the U6 promoter, a type III RNA polymerase III promoter commonly used to drive the expression of small hairpin RNA (shRNA) in RNA interference (RNAi) vectors. The vector was digested with BbsI (Thermo Fisher Scientific, #ER1011) to prepare it for cloning. Two annealed oligos, designed based on the target site sequence (20 bp) and followed by a 3 bp NGG PAM sequence, were then cloned into the vector before the sgRNA scaffold. These oligos were selected using the CRISPOR tool (Version 5.01) to ensure high specificity, indicated by a high MIT specificity score and minimal predicted mismatches (Hsu et al., 2013). Following the cloning process, the PX459-CYFIP2-KO DNA plasmid was purified by transforming it into the Stbl3TM Chemically Competent E. coli strain (Thermo Scientific, #C737303). The purified plasmid was then used to transfect the SH-SY5Y cell line (ATCCTM, CRL2266) using LipofectamineTM 3000 (Thermo Fisher Scientific, #L3000001) according to the manufacturer's protocol.

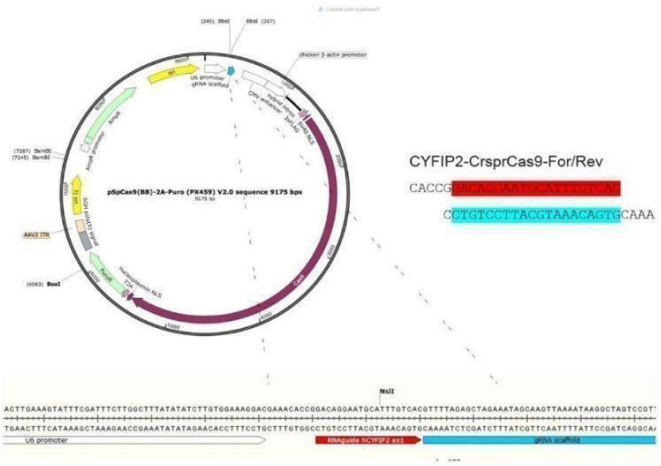

Figure 3.3: Eukaryotic expression vector SpCas9(BB)-2A-Puro (PX459) V2.0 used to generate CrispR/Cas9 KO cell lines.

To eliminate untransfected cells, we first determined the optimal selection antibiotic concentration by performing a kill curve on WT SH-SY5Y cells using increasing concentrations of puromycin (Sigma-Aldrich®, #P9620), as detailed in table 6. Transfected cells were then subjected to antibiotic selection by treating them with 2 ng/µl puromycin for 24 hours.

Puromycin conc. ng/µl	**10.0**	**7.0**	**4.9**	**3.4**	**2.4**	**1.7**	**1.2**	**0.8**	**0.6**	**0.2**	**0.0**
% of live cells	*0*	*0*	*0*	*0*	*0*	*0.4*	*2*	*30*	*70*	*100*	*100*

Table 6 : Pyromycin dose response kill curve

After total RNA extraction, the target region of the CYFIP2 gene for Cas9 was sequenced to confirm the presence of genome editing. The generated cDNA from the reverse transcription (RT) reaction was PCR-amplified using intronic primers flanking the target region of genome editing, as shown in Table 6. Sanger sequencing was performed on the PCR products, and the resultant electropherogram was analyzed using the ICE Analysis tool (Syntego)

nt-hDNA-CYFIP2-For	AGATGAAAGGTGGACGCAGCA
Int-hDNA-CYFIP2-Rev	ATGCCTCTGGTGTGAGAAGC

Table 7: List of primers used to amplify the cyfip2 intronic region flanking the exon1, target of genome editing.

5.2 Generation of SH-SY5Y KI CYFIP2 and R87C

To generate a stable population of CYFIP2 WT and mutation R87C (SH-SY5Y knock-in (KI) cell lines), we utilized a multiplicity of infection (MOI) of 1. Lentiviral particles were produced using transgenic vectors pRRLSIN.cPPT.PGK-hCYFIP2-HA. WPRE, pRRLSIN.cPPT.PGK-R87C-HA. WPRE, as previously described. These lentiviral particles were then directly added to the culture medium of SH-SY5Y CYFIP2 knockout (KO) cell lines (previously generated by using CrisperCas9 tecnology as described above) This approach ensures the efficient introduction and stable expression of the CYFIP2 KI or R87C variants within the SH-SY5Y cell population.

6.1 Generation of hippocampal *CYFIP2*/R87C *KI* model. Production of lentiviral vector to downregulate CYFIP2 protein

Vectors to reduce endogenous CYFIP2 protein were constructed using the TWEEN-Lenti vector (7970bp), which contains the Green Fluorescent Protein (GFP) coding sequence controlled by the hPGK promoter, generously provided by Prof. Leonardo Elia (University of Brescia). The shRNA sequence is expressed under the control of the H1 promoter. After the vector was double-digested with XbaI and XhoI (#ER0681; #ER0692 Thermo Fisher Scientific), two annealed oligonucleotides containing the palindromic shRNA sequence targeting CYFIP2 mRNA were cloned. The shRNA sequence, designed to recognize the 3'UTR region of the mouse CYFIP2 transcript at position 3775, was created using the shRNA Optimal Design tool from Kay Lab (https://med.stanford.edu/kaylab). Following cloning, Stbl3TM Chemically Competent E. coli strain (#C737303 Thermo ScientificTM) was transformed to isolate the TweenLentiH1-sh3775-Cyfip2 DNA plasmid Figure 3.4 Eukaryotic expression vector TweenLentiH1-sh3775-Cyfip2 used to downregulate CYFIP2 protein in hippocampal culture.

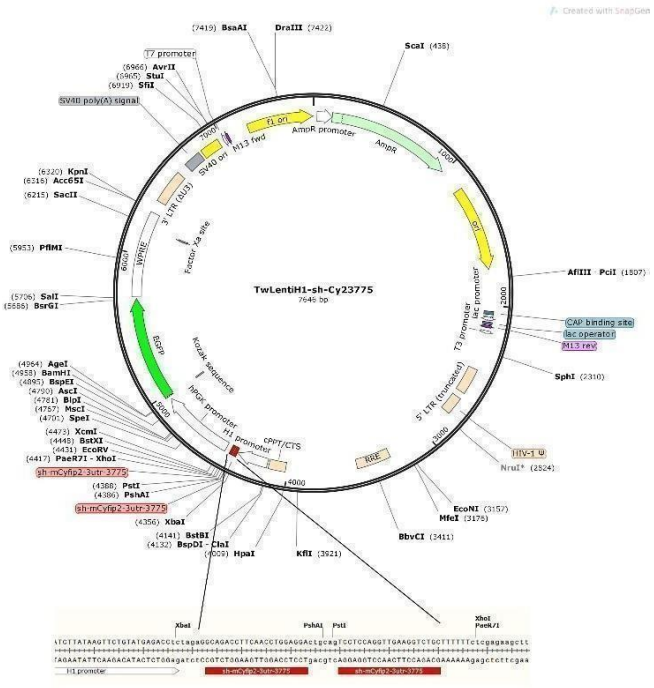

Figure 3.4: Eukaryotic expression vector TweenLentiH1-sh3775-Cyfip2 used to downregulate CYFIP2 protein in hippocampal culture.

6.1.1 Lentiviral transduction of hippocampal cells

In order to generate a CYFIP2 /R87C KI model, hippocampal cultures at DIV1 were transducted adding a mix of lentiviral particles containing TweenLentiH1-sh3775-CYFIP1 and CYFIP2 to downregulate endogenous CYFIP1 and CYFIP2 protein and pRRLSIN.cPPT.PGK-hCYFIP2-HA.WPRE, pRRLSIN.cPPT.PGK-R87C-HA.WPRE to induced the expression of CYFIP2/KI or R878C variant. PFA 4% were used to fix neuronal cultures at DIV3 or DIV18. The fixed cells then were used to assess axon development or spine frequency.

7.1 Confocal microscopy

Fluorescently labeled cells were captured using an inverted laser scanning confocal microscope (LSM900, Carl Zeiss, Jena, Germany) equipped with a 20x objective, achieving a resolution of 3964 x 3964 pixels. The images captured represent maximum intensity projections (MIP) of 15 consecutive optical sections, with 3 Z sections spaced at 1.5 µm intervals. The Simple Neurite Tracer tool from Fiji (Schindelin et al., 2012) was used to measure total path length and the number of branches. For this kind of analysis, a minimum number of 60 cells was used for both conditions. Whereas spine density was assessed by manually counting the spines within a 10 µm dendritic segment using ImageJ. We examined the number of the spines in at least three secondary dendrites for a minimum of 15 cells for each condition.

8.1 Statistical analysis

The data were displayed using the standard error of mean (SEM) or mean. GraphPad Prism version 8 (GraphPad Software inc., USA) was used to evaluate the data statistically. Unpaired t-test was used to analyze the morphological changes of Cyfip2 WT and R87C in both primary hippocampal neurons and SH-SY5Y neuroblastoma cell line, as well as protein degradation assay. One way ANOVA followed by Tukey's post hoc test or Newman-Keuls multiple comparison was applied for the other data. Statistical significance was assumed at $p<0.05$.

4. RESULTS

3.1. Protein degradation

Alterations in signal transduction machinery are frequently observed in many neurodevelopmental disorders. For this reason, we investigated whether the levels of the R87C-mutated version of CYFIP2 protein might be affected. After transfecting equal amounts of plasmid into HEK293T cells, we observed a reduction in protein expression levels for the R87C mutant.

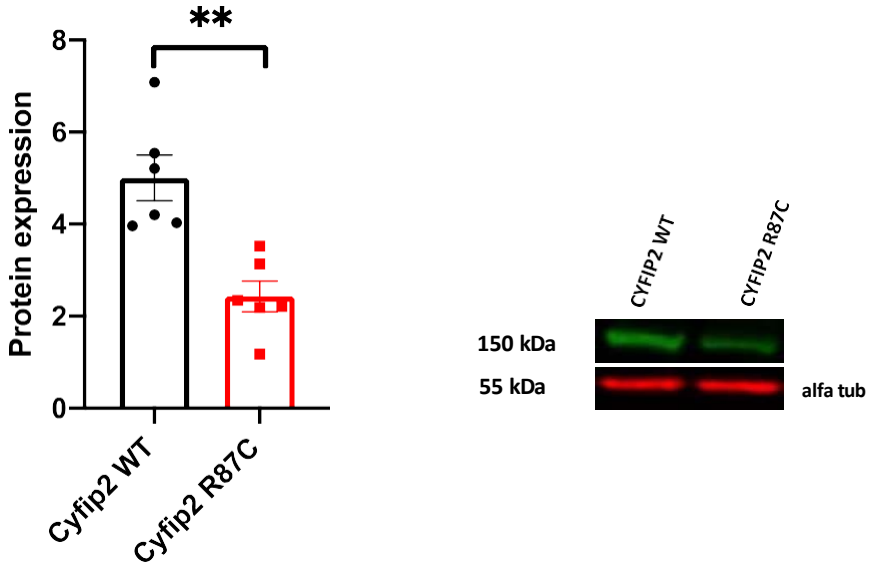

*Figure 4.1: Graph showing the expression levels of CYFIP2 and R87C: The infrared (IR) acquisition of the western blot results, obtained from cellular lysates of HEK293T cells transfected with CYFIP2 and R87C, shows the relative expression levels of each protein. The signal was revealed using a rabbit-α-HA tag antibody, targeting the HA-tagged CYFIP2 and R87C variants in the lysates. (Nr=6 for WT, Nr=6 for R87C) Unpaired T-test **<0.01.*

This experiment demonstrated a reduced level of expression of the mutated variant compared to WT, which aligns partially with in vivo data. In fact, Han and colleagues generated heterozygous mice carrying the R87C variant and observed reduced levels of CYFIP2 in the mutant mice compared to WT. (Kang et al., 2023).

3.2 Anisomycin treatment and evaluation of protein degradation

Since we observed a reduction in the expression of the mutated variant R87C, we hypothesized that this reduction might be due to either decreased translation or increased degradation. To test this, we transfected HEK293T cells with plasmids encoding CYFIP2 and R87C variant, and then treated the cells with anisomycin (40 µM), a potent inhibitor of translation, which allowed us to assess the degradation rate of the proteins. We harvested the cells at different time points: at time zero (before treatment), after 4 hours and after 8 hours of anisomycin treatment. We then performed Western blot analysis to evaluate the expression pattern over time. As shown in the graph below, we observed a trend of a higher degradation rate of the mutated R87C variant compared to the CYFIP2. This experiment demonstrates that probably the reduced expression level of R87C variant may be due to a higher speed of degradation.

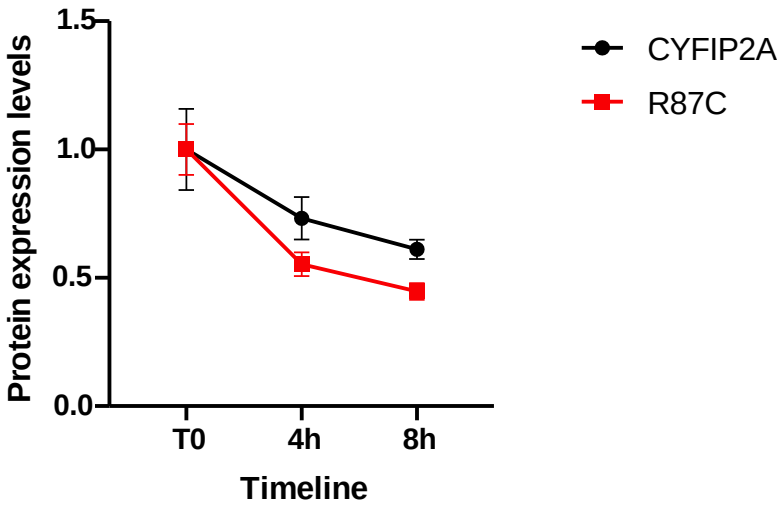

Figure 4.2: Western blot analysis: Expression levels of CYFIP2 WT and mutated variant R87C over time, after treatment with 40 µM *anisomycin and extraction of proteins at different time points.*

3.3 Crisper Cas 9 technology: Generation of KO SH-SY5Y cell line

After gathering some preliminary data using the NIH3T3 cell line, the next step was to advance the study by employing a model that more closely resembles a neuronal phenotype. For this reason, we selected the neuroblastoma SH-SY5Y cell line as an *in vitro* model because of its capability to migrate, proliferate, and differentiate into cells with neuronal characteristics. Using SH-SY5Y allows us to investigate CYFIP2 WT as well as the mutated variant CYFIP2 R87C role in cell morphology, as well as to replicate their progression into a neuronal phenotype by inducing their differentiation with a specific medium.

First, as reported in the material and methods section, we established an SH-SY5Y KO cell line that is deficient in both CYFIP2 alleles (CYFIP2−/−) by taking advantage of the recently developed CRISPR- Cas9 technology (Cong et al., 2013). Subsequently through the transduction of lentiviral particles carrying the whole CDS of human CYFIP2 WT/R87C forms, CYFIP2 KI and mutated variant CYFIP2 R87C cell lines were generated.

The SH-SY5Y CYFIP2 KO cell line was produced by transfecting WT cells with the Feng Zhang-created plasmid px459 (SpCas9(BB)-2A-Puro (PX459) V2.0) (Ran et al., 2013), in which the RNA guide sequence that recognizes the first exon of the endogenous CYFIP2 gene was previously cloned. This plasmid carries the expression of Cas9 from S. pyogenes with 2A-Puro and Single Guide RNA (V2.0) which consists of 76 nt of scaffold, required for Cas-binding and 20 nt of spacer that identifies the genomic target to be changed. The expression of sgRNA is under the control of U6 promoter, a type III RNA polymerase III promoter commonly used for driving small hairpin RNA (shRNA) expression in vector-based RNAi. Once produced in the cell, sgRNA molecules drive Cas9 enzymes to his target sequence located on the first exon of *Cyfip2* gene and carry out a double-strand break (DSB) within the target DNA (Fig. 4.3). The resulting DSB is then repaired by one of two general repair pathways: the efficient but error-prone non-homologous end- joining (NHEJ) pathway, or the less efficient but high-fidelity homology directed repair (HDR) pathway. The NHEJ repair pathway is the most active repair mechanism, and it frequently causes small nucleotide insertions or deletions (indels) at the

DSB site. The randomness of NHEJ- mediated DSB repair has important practical implications, because a population of cells expressing Cas9 and a gRNA will result in a diverse array of mutations. In most cases, NHEJ gives rise to small indels in the target DNA that result in amino acid deletions, insertions, or frameshift mutations leading to premature stop codons within the open reading frame (ORF) of the targeted gene. The design of gRNA, created using CRISPER tool (Concordet and Haeussler, 2018), was complementary to the exon 1 of the target site sequence. Plasmid DNA carrying the expression of gRNA, Cas9 protein and puromycin resistance was transfected in SH-SY5Y cell line. After antibiotic selection, total RNA of cells was purified, retrotranscribed and amplified using the intronic primers flanking the target region of genome editing and sequenced, to evaluate whether genome editing was present.

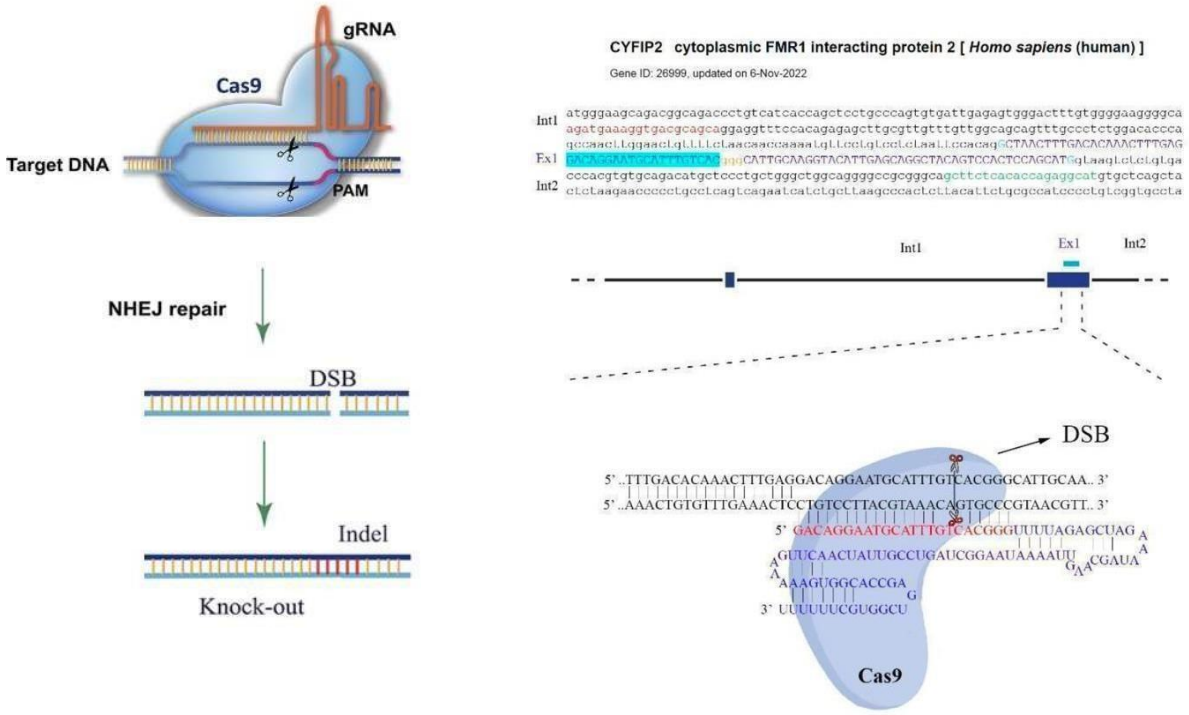

Figure 4.3: A schematic illustration of the CRISPR/Cas system. Double-strand breaks (DSBs) are created and subsequently repaired by the cell's own DNA repair machinery through the error-prone non-homologous end joining (NHEJ) pathway. This repair process can lead to random insertion or deletion (indel) mutations at the break site. These indel mutations may result in gene knockout if they induce a frameshift and an early stop codon within the coding region of the gene (Left). Highlighted in cyan is the single guide RNA (sgRNA) target sequence, followed by a GGG protospacer adjacent motif (PAM), located in the first exon of the human CYFIP2 gene. The double-strand break, induced by the Cas9 protein on the CYFIP2 gene (black sequence), occurs after the sgRNA (red sequence) recognizes and binds to the target site (Bottom, right). This schematic is adapted from Ran et al., 2013.

After Sanger sequencing, the resultant electropherogram was assessed using the ICE Analysis tool (Syntego© https://ice.synthego.com/#/), a software that offers fast and reliable analysis of CRISPR editing data. After analysis, we obtained 96% of indel mutations with the same percentage of *KO* score (Fig. 4.4, top). The results showed a large prevalence of the same mutation; in particular, 73% of molecules presented an insertion of one Thymine (+1). The other most represented mutations are all deletions: -1 (11%); -2 (6%); -7 (2%) (Fig. 4.4, bottom).

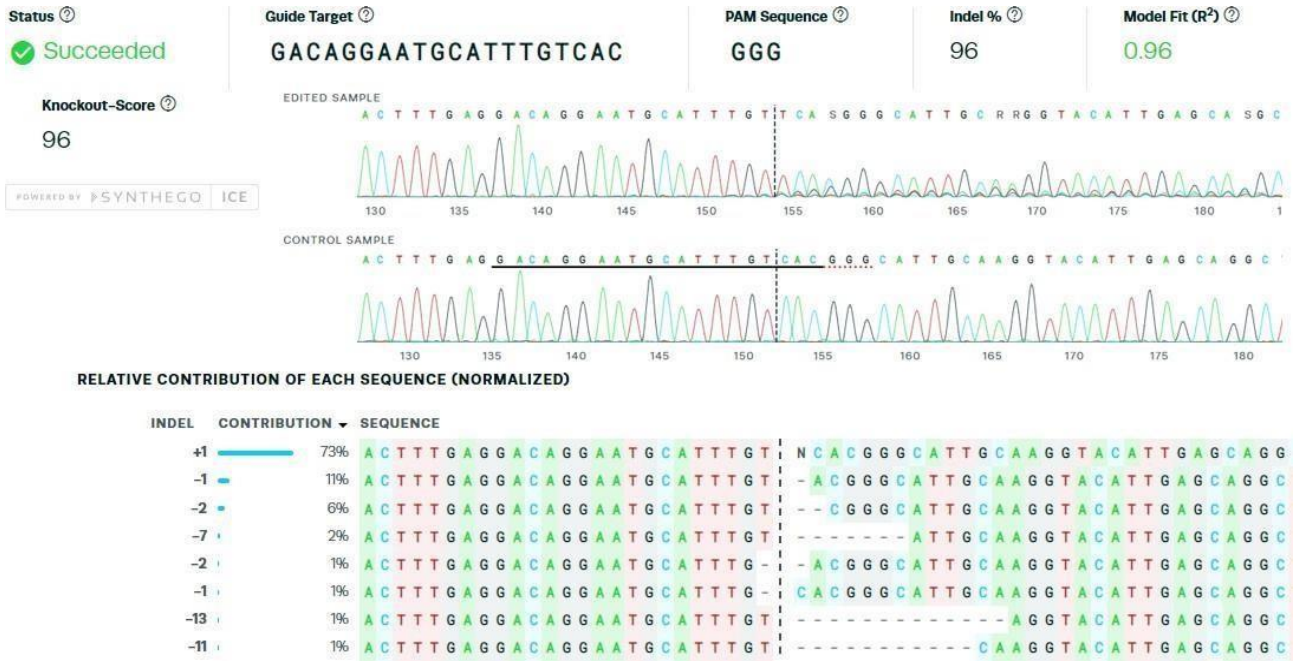

Figure 4.4: Output obtained from Syntego© ICE Analysis tool. Comparison of electropherograms of the sgRNA recognition sequence (black underlined), obtained from sequencing of edited and WT samples (top). Alignment of different sequences present in the edited sample with relative contribution in percentage (bottom)

These data demonstrate that the Crispr-CAS9 approach is highly efficient. If the detected mutations are translated into proteins, they cause premature stop codons and frameshift. The complete absence of wild-type (WT) sequences and the exclusive presence of only frameshift mutations, confirms the successful creation of a homozygous CYFIP2 knockout (KO) cell line.

Following that, we performed a western blot analysis to verify the absence of protein in the KO generated SHSY5Y cell line. As it is shown in the below image, there is no presence of CYFIP2 in the KO SHSY5Y cell line.

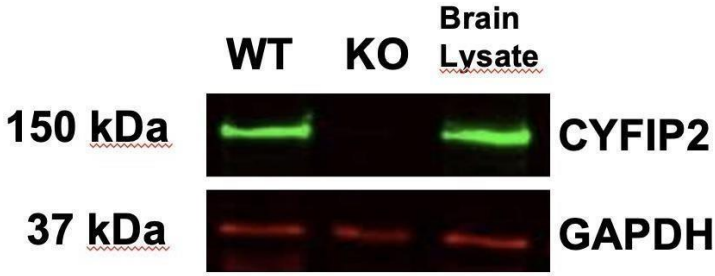

Figure 4.5: Western blot analysis confirming the generation of KO SHSY5Y cells using Crisper-Cas9. IR acquisition of WB obtained from cellular lysate derived from WT SH-SY5Y cell line (WT), cellular lysate from SH-SY5Y cell line after CRISPR/Cas9 and puromycin selection (KO) and mouse brain lysate as a positive control. Endogenous CYFIP2 proteins are detected using rabbit-α-CYFIP2 antibody.

3.4 Phenotypic alteration of SH-SY5Y *CYFIP2 Knock-Out* cell line

Plasma membrane blebbing is a cellular process triggered by a combination of events that involve local disruption of interactions between the membrane and the actin cortex, leading to the rapid protrusion of the plasma membrane, associated with the appearance of cell blebs. These structures are defined by a bulging of the plasma membrane, creating a large, nearly spherical distortion on the cell surface (Charras et al., 2005). Numerous studies in the literature have shown that interference with lamellipodia formation encourages plasma membrane blebbing. Inhibition of lamellipodia by blocking WRC or Arp2/3 complex functionality induces plasma membrane blebs in various cell types across different organisms (Suraneni et al., 2012). Considering the role of CYFIP2 in actin dynamics thus, cytoskeleton organization, this preliminary experiment aimed to characterize the phenotypic effects of its absence. As it is demonstrated in the figure 4.6 SH-SY5Y WT cells exhibit non-polarized cell bodies characterized by a neuroblast-like phenotype with a few shortened processes, whereas SH-SY5Y CYFIP2 KO cells show a significant morphological change, with the formation of cell blebs on the plasma membrane.

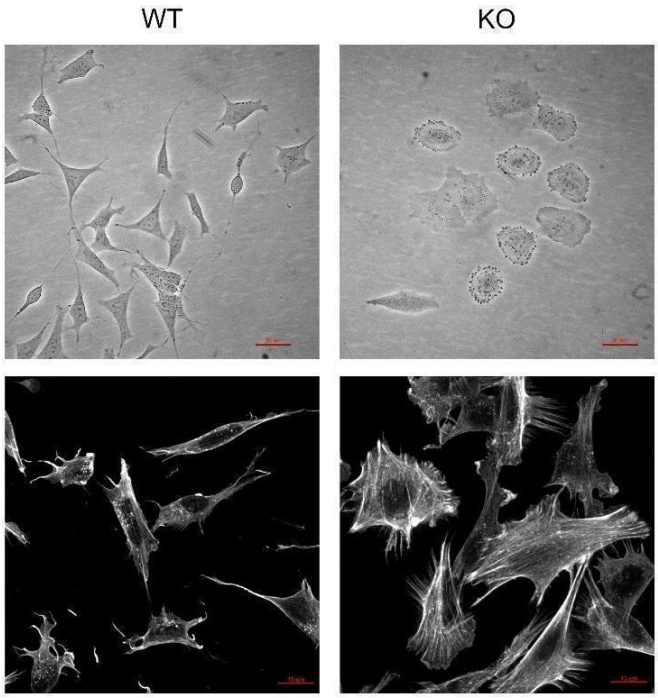

Figure 4.6: Morphological alteration of SH-SY5Y cell line after CYFIP2 gene knocking out. Phase contrast microscopy images of SH-SY5Y WT (top, left) and SH-SY5Y KO (top, right) (Optech Biostar IB 20X scale bar: 30 µm). Phalloidin staining of SH-SY5Y cell line WT (bottom, left) and CYFIP2-KO (bottom, right) (Zeiss© LSM880 40X scale bar: 15 µm).

LSM confocal microscopy was used to evaluate the F-Actin filaments organisation, after fixation and staining with Alexa FluorTM 647 Phalloidin conjugated probe. As can be observed at the bottom of the figure 4.6, KO cells showed a completely different actin filaments organisation compared to WT cells. This experiment underscores the crucial role of the CYFIP2 protein in maintaining cytoskeletal organization, a process closely linked to the regulation of actin dynamics.

3.5 Generation of KI CYFIP2/ R87C in KO SH-SY5Y cell line

To get insight into the role of R87C variant in actin dynamics which directly may impact cell morphology and subsequently cell function, we generated a stable KI CYFIP2 and KI R87C cell line by starting from SH-SY5Y KO cell line.

First, we produced lentiviral particles containing the *CYFIP2* and R87C variants, cloning in a backbone from 3rd generation lentiviral vector pRRLSIN.cPPT.PGK-GFP.WPRE, the human CDS of *CYFIP2* gene (NM_001037333.3). Then the cells were transduced with high MOI to produce stable populations of SH-SY5Y *CYFIP2* KI cells.

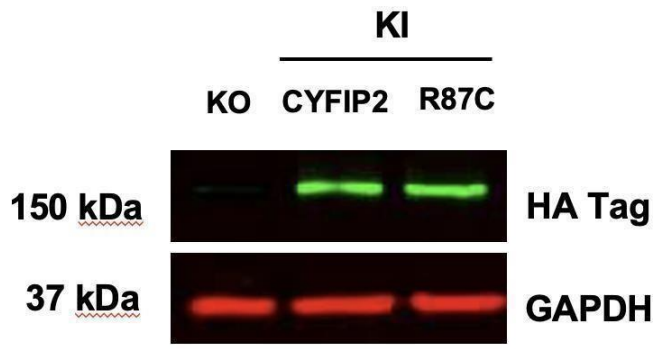

Figure 4.7: IR acquisition of WB obtained from cellular lysate derived from KO SH-SY5Y cell line (KO), and KI SH-SY5Y CYFIP 2 and R87C samples. Exogenous CYFIP2 proteins are detected using rabbit-α-HA antibody.

Western blot analyses were performed to check the presence of KI on this cellular line. As it is reported in the image 4.7 the KI was obtained for both CYFIP2 and its mutated variant R87C. The presence of both exogenous proteins CYFIP2 KI and R87C was revealed by using antibody against HA tag.

3.6 Evaluation of morphological feature of CYFIP2-WT, KO and KI SH-SY5Y cell lines

CYFIP2, as a member of the WAVE regulatory complex (WRC), plays a crucial role in modulating actin rearrangement in various cellular contexts. The dynamics of actin polymerization are essential for numerous cellular processes, including cytoskeletal reorganization, membrane-based protrusions, and the formation of specialized structures such as axonal growth cones and dendritic spines. Given CYFIP2's active involvement in actin dynamics, we utilized our KO SH-SY5Y model to investigate the morphological features that may be impacted by altered actin dynamics. After successfully generating the CYFIP2 knockout (KO) SH-SY5Y cell line and establishing a stable knock-in (KI) line, we sought to explore the role of CYFIP2 by comparing the morphological characteristics of these models. This experiment provides insights into the effect of CYFIP2 deficiency on cell morphology, particularly those features dependent on actin regulation, such as cell area, aspect ratio as well as integrated density which is a parameter linked with the amount of f-actin presented in a cell.

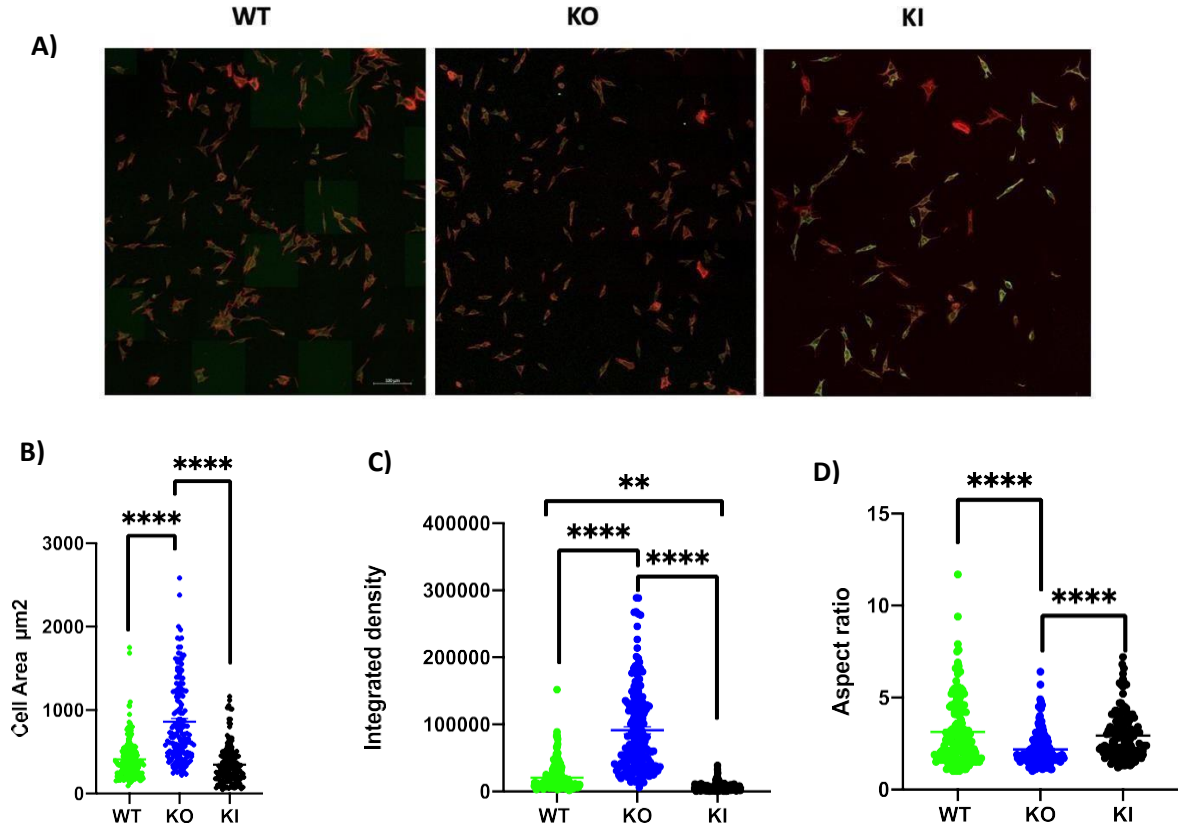

*Figure 4.8: Morphological analysis of WT, KO, and KI in SH-SY5Y cell lines. The different morphological parameters (cell area, Phalloidin Intensity, Aspect Ratio) have been analysed with ImageJ software. (Nr=153 for WT, Nr=162 for KO, Nr=139 for KI.) One-way ANOVA followed by Tukey's multiple comparisons: **<0.01 ****<0.0001.*

As it is demonstrated in the figure 4.8, we observed significant differencies in all parameters measured among WT and KO cell line; interestingly, this modifications were rescue by the overexpression of CYFIP2. Particularly we obseved an increase in cell area in the KO cell line, which was restored in the KI model. The same pattern has been observed also for aspect ratio as well as integrated density which is a parameter used to measure the amount of F-actin. These data suggest a key role of CYFIP2 in cell morphology which are consequnces of its role in actin dynamics.

3.7 Evaluation of morphological features between CYFIP2-KI and R87C SH-SY5Y cell lines

Further we evaluate the effect of the R87C variant on the same morphological parameters analysed above, using the KI as a control. As mentioned previously, we began by generating a CYFIP2 KO line and subsequently established a stable SH-SY5Y cell line expressing exogenous CYFIP2 along with the R87C mutation.

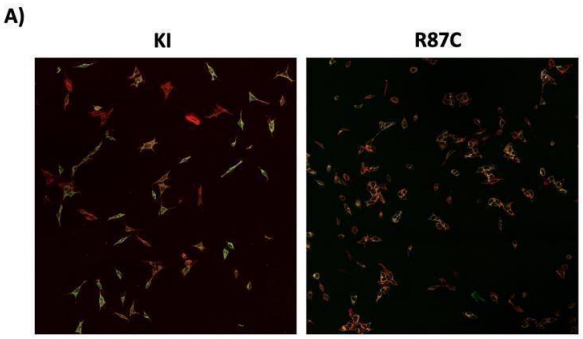

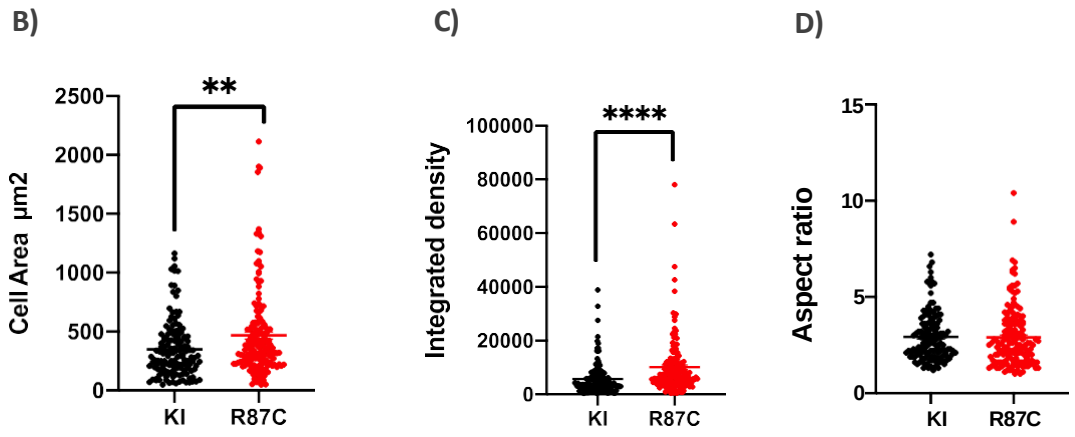

*Figure 4.9: Morphological analysis of KI and R87C variant in SH-SY5Y cell lines. The different morphological parameters (cell area, Phalloidin Intensity, Aspect Ratio) have been analysed with ImageJ software. (Nr=139 for KI, Nr=159 for R87C). Unpaired T-test: **< 0.01 ****< 0.0001.*

In this experiment we observed diferencies between KI and R87C variant regarding, cell area and integrated density. Particularly we obseved a significant increse of both parameters in R87C variant. Considering aspect ratio we didn't observe any differencies between the two cellular population.

3.8 Neurite development during CYFIP2-WT, KO and KI SH-SY5Y differentiation

Since CYFIP2, is predominantly found in neurons (Zhang, Lee and Han, 2019) and has been associated with various neurodevelopmental disorders, we aimed to explore its role in neuronal differentiation, a key process in neurodevelopment. SH-SY5Y is a cellular line with similar neuronal phenotype, which under specific treatment can be induced the differentiation. Indeed, this cellular line has been well established as a model of neuronal differentiation. The cells undergo the process of differentiation by supplementing the medium with Retinoic Acid (RA) and brain derived-derived neurotrophic factor (BDNF). (Hromadkova et al., 2020).

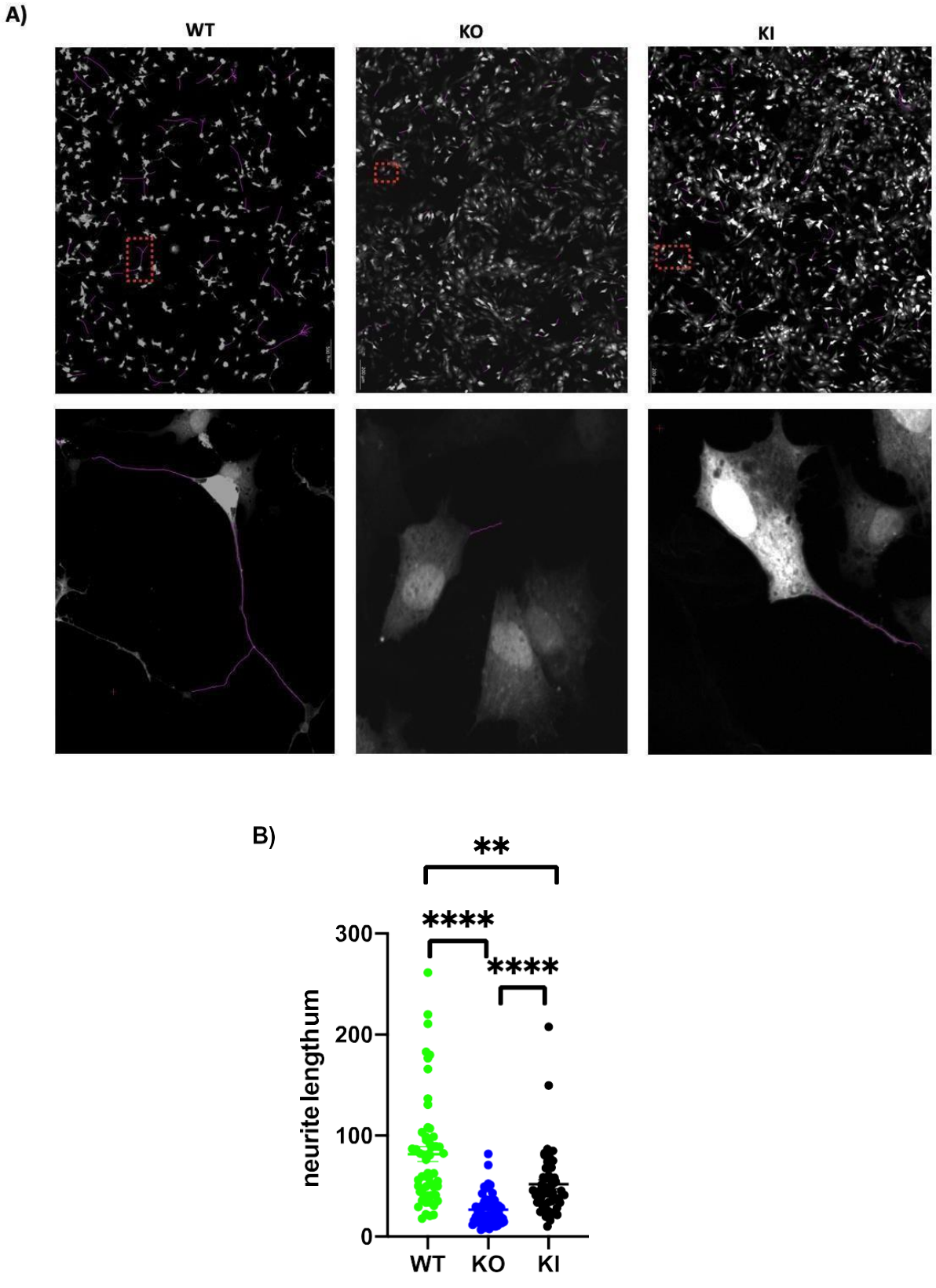

*Figure 4.10: Neurite tracing of different populations of SHSY-5Y of cells by using Simple Neurite Tracing plug in. (Nr=59 for WT, Nr=62 for KO, Nr=57 for KI) One-way ANOVA followed by Tukey's multiple comparisons:**< 0.01 ****< 0.0001. Test analysis showed that CYFIP2 KO cells do not develop a neural-like morphology visible in WT population. The length of neurite was different between KO cells and other populations of cells as reported in the graph.*

By using the ImageJ's framework Simple Neurite Tracer (SNT), we measured the length of neurite in the cells. In this experiment we observed that CYFIP2 KO cells have lost their ability to produce a characteristic neurite-like morphology after differentiation compared to WT. This effect has been reversed in the KI cell line; indeed, the ability of neurite development is partially restored in *CYFIP2 KI* cell population. This experiment highlights the important role of CYFIP2 in neuronal differentiation in SH-SY5Y model.

3.9 Neurite development during CYFIP2-KI and R87C

Following the characterization of neuronal differentiation in the SH-SY5Y model across WT, KO, and KI cells, we repeated the experiment to examine the differences between the KI and R87C cell lines. As previously performed, SH-SY5Y cell differentiation was conducted in two stages using distinct medium: the first one supplemented with Retinoic Acid (RA) and the second with Brain-Derived Neurotrophic Factors (BDNF). In this experiment, we observed a reduced differentiation capacity in the population of cells carrying the R87C mutation. The R87C cell line, overall, exhibited shorter neurites compared to its counterpart KI CYFIP2.

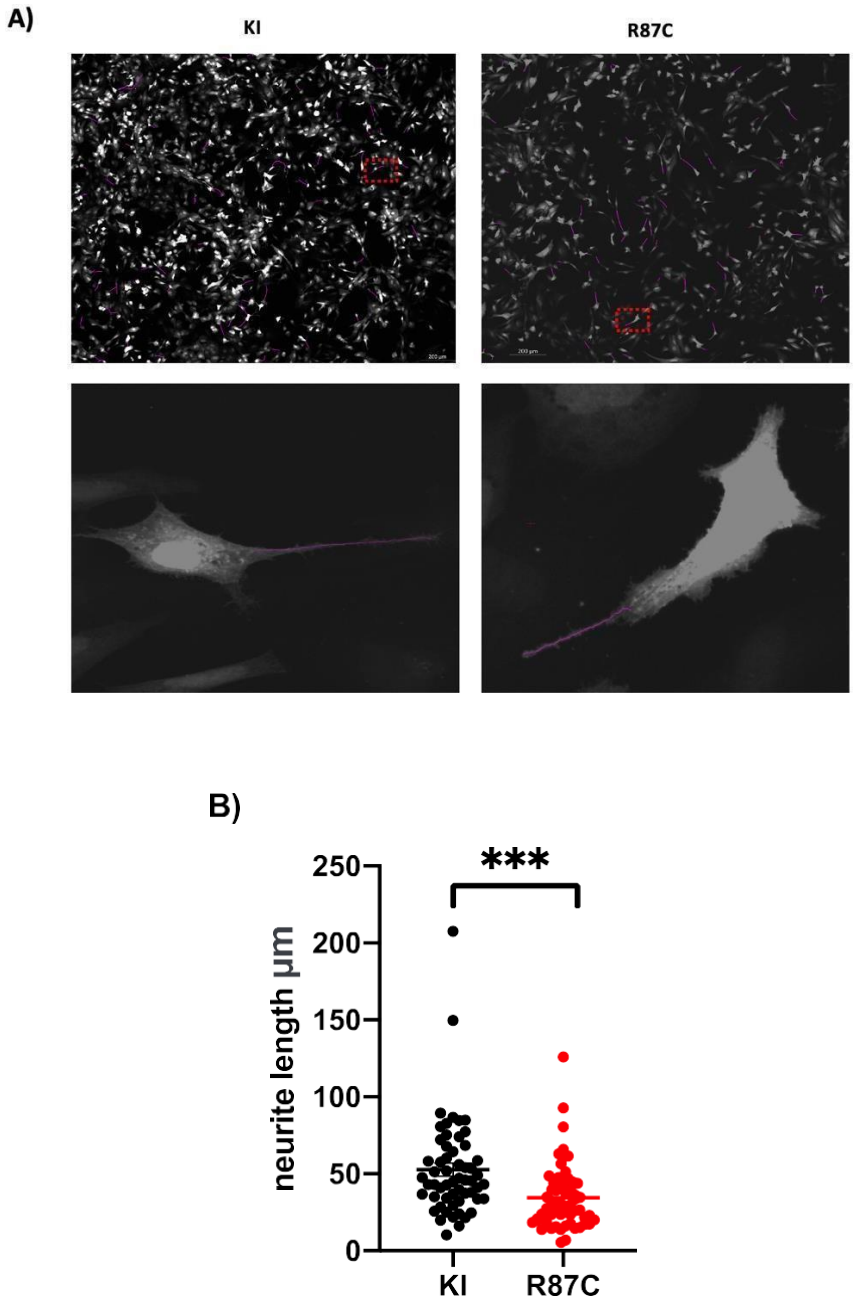

Figure 4.11: A) Neurite tracing of different populations of SH-SY5Y of cells by using Simple Neurite Tracing plug in.

B) T- test analysis showed that R87C cells does not develop a neural-like morphology in the same way as KI population. (Nr=57 for KI, Nr=58 for R87C, Unpairtesd T-test ***<0.001.

3.10 Generation of a murine hippocampal primary neuronal model

By employing the SH-SY5Y cell line, known for its neuronal-like properties, we gained significant insights into the role of Cyfip2, including its absence and the mutated R87C variant, in various cellular processes discussed previously. However, this model has its limitations, and to address them, we utilized murine primary hippocampal cell cultures, which provide a more suitable model for these types of studies. First, we aimed to down-regulate the expression of the endogenous CYFIP1 and CYFIP2 protein, we transduced primary hippocampal neuronal cultures at DIV1 with lentiviral particles containing a shRNA targeting the 3'UTR of both *Cyfip1* and *Cyfip2* gene.

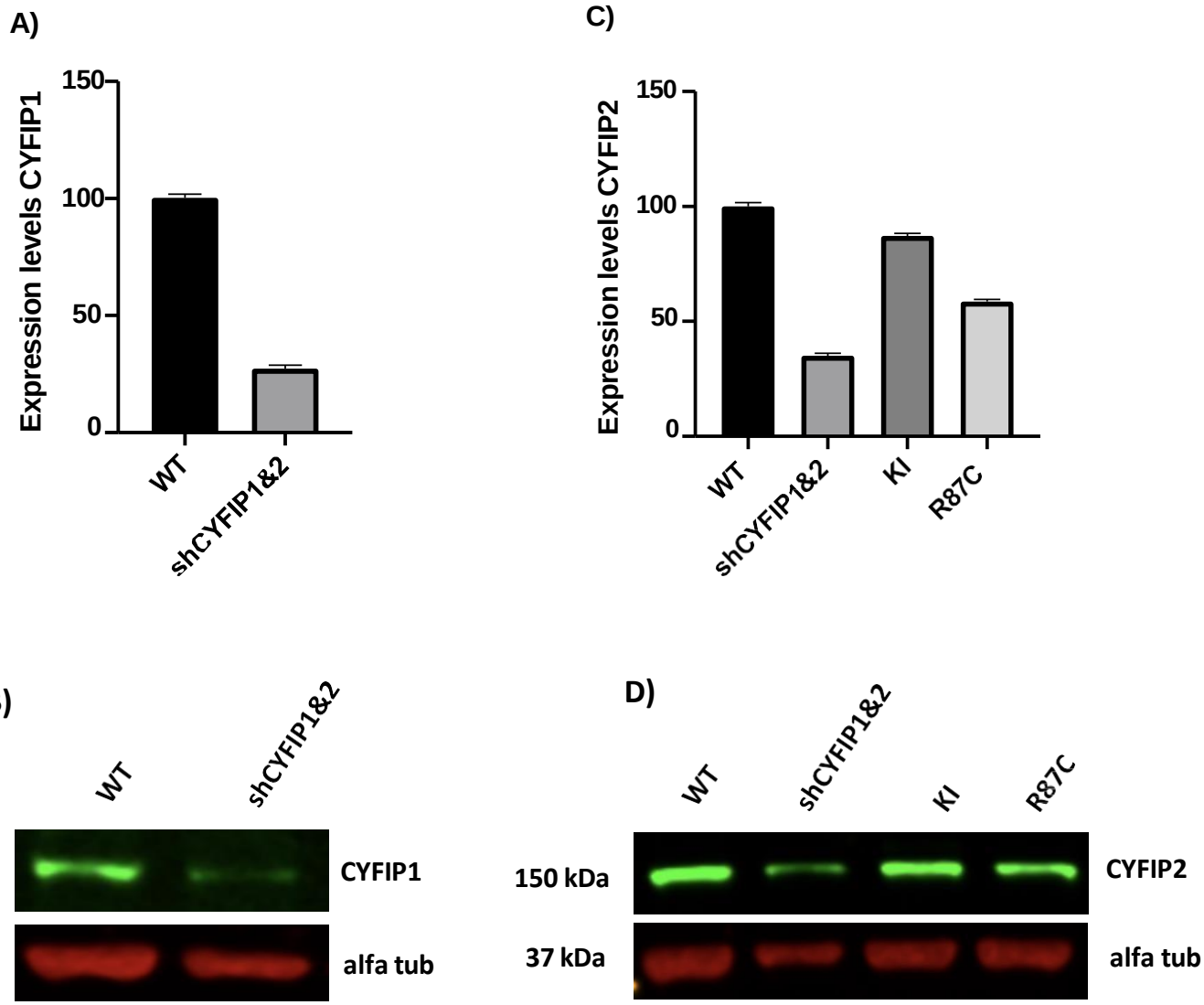

Figure 4.12: Western blot analysis obtained from cellular lysate of WT primary hippocampal cells (WT) and after Lentiviral transduction of shRNA targeting the 3'UTR of CYFIP1 and CYFIP2 gene. A) Graph showing the percentage of reduction of CYFIP1 after downregulation, B) Detection of endogenous Cyfip1 by using rabbit anti CYFIP1 antibody and alfa tub as housekeeping. C) Graph showing the percentage of downregulation of CYFIP2 and the expression levels of KI CYFIP2 and R87C. D) Detection of CYFIP2 protein by using rabbit anti CYFIP2 antibody and alfa tub as housekeeping.

To confirm the efficiency of gene silencing for both CYFIP1 and CYFIP2, we conducted a western blot analysis to assess protein expression levels. As shown in figure 4.12 A, 48 hours post-transduction, endogenous CYFIP1 protein levels were reduced by approximately 70%, with a similar reduction observed also for CYFIP2 figure 4.12 C The silenced cells were co-transduced with lentiviral particles expressing either CYFIP2 or the R87C variant (Figures 4.12 C and D) for the further studies.

3.11 Study of axon development of hippocampal primary neurons

Studies in zebrafish evidence the role CYFIP2 in axonal cone growth. By integrating the molecular replacement strategy and time sequenced tracking of axon elongation Cioni JM and colleagues demonstrated an involvement of CYFIP2 in this process.

Particularly, in response to contact axon-axon CYFIP2 was translocated to the outgrowth cone to manage the filopodial dynamics thus to induce axonal sorting or repulsion. Deletion of Cyfip1 and CYFIP2 with CRISPER-Cas9 caused impairment in axonal growth. This line of evidence suggested an implication of CYFIP1 in axonal growth and CYFIP2 in axonal sorting (Cioni et al., 2018).

Based on this finding as well as in the results we obtained in SH-SY5Y differentiation we aimed to study the axon growth in neurons in early stages in vitro. Specifically hippocampal neurons at DIV1, were co-transduced with lentiviral particles expressing the CYFIP2 variant along with lentivirus carrying shRNA to knock down endogenous CYFIP1 and CYFIP2 protein. In this experiment we evaluated the axon development between three different population of neurons: WT, KD and KI CYFIP2. After 72 hours, the cells were fixed and images comprising a grid of 20x20 frames were captured at 40X magnification using a Zeiss© LSM 900 confocal microscope. By using

Simple Neurite Tracer (SNT) (Arshadi et al., 2021), an ImageJ's plug-in for analyses of neuronal morphology, we plotted a minimum of 60 neural axons for each population of cells (Figure 4.13). From this analysis we measured three different parameters: the number of branches, total axon length and complexity index (a function of neurite attachment points and ending points).

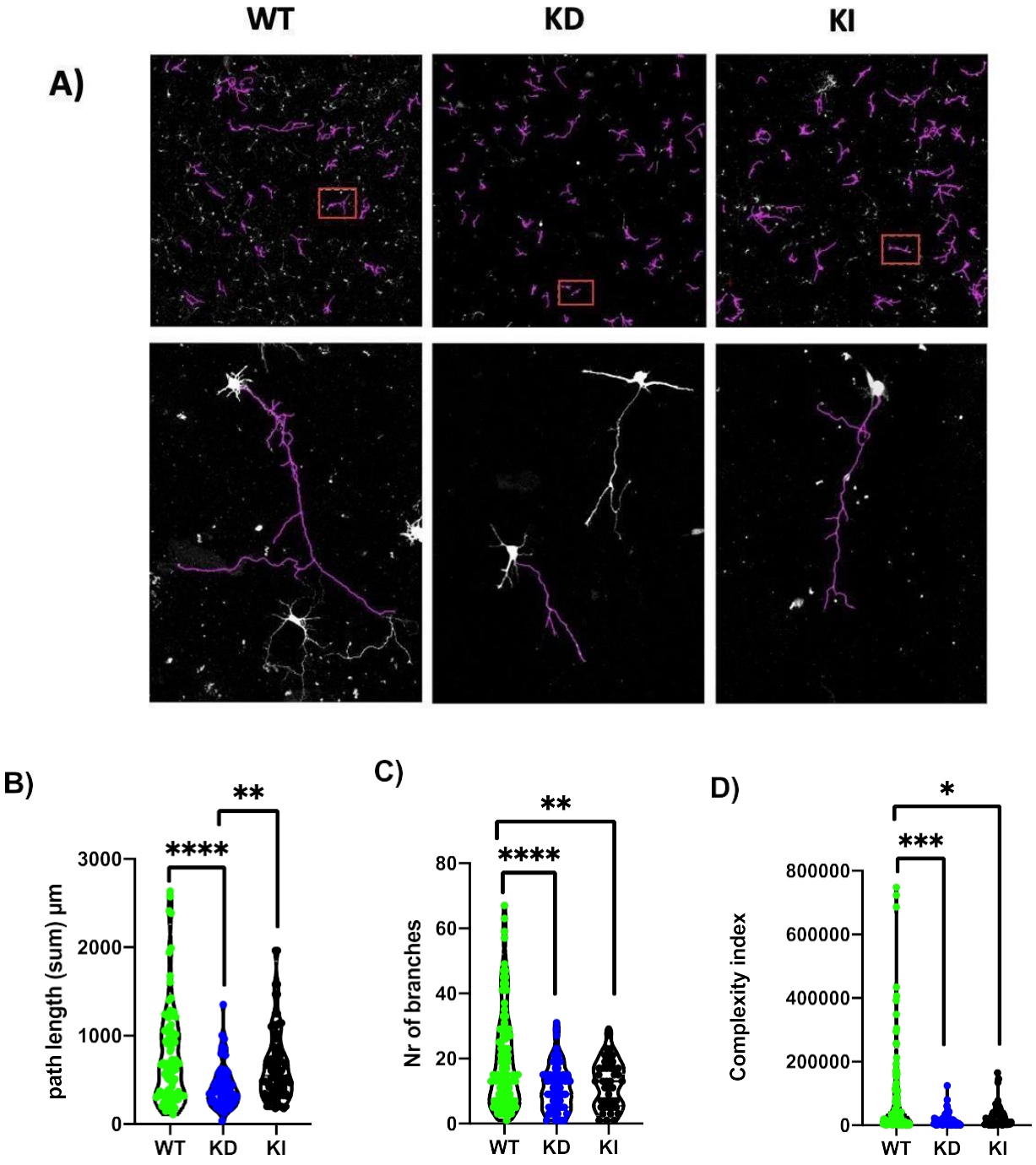

Figure 4.13: A) Axon tracing of hippocampal culture at DIV3 by Simple Neurite Tracing in purple (Top). The complexity of axonal arborization wasdetermined by analysing the total length of axons thenumberof branches, and the complexity

index. (Nr = 97 (WT), 61(KD) 44(KI), Tukey's multiple comparisons test: * <0.05 ** <0.01 ***<0.001 ****<0.0001*(Figure 4.13 B,C,D).*

In this experiment we observed a decrease of path length, number of branches as well as overall complexity index in KD population compared to WT. Intriguingly, this decrease was observed also for KI population of neurons.

Further we examined the same exact parameters also between KI an R87C mutation.
Hippocampal neurons at DIV1, were co-transduced with lentiviral particles expressing the CYFIP2 or R87C variant along with lentivirus carrying shRNA to knock down endogenous CYFIP1 and CYFIP2 protein, aiming to examine the effects of R87C alterations without the influence of the native protein. After 72 hours, the cells were fixed and images comprising a grid of 20x20 frames were captured at 40X magnification using a Zeiss© LSM 900 confocal microscope. In this experiment we observed a statistically significant difference between, *CYFIP2 and* neurons carrying R87C variant in each of the three parameters considered (Unpaired T-Test - N° of branches; Path length [sum] µm; Complexity Index log2: $p<0.0001$). Unpaired T-test showed a reduction in the N° of branches and Path length as well as complexity index in neurons carrying the mutation.

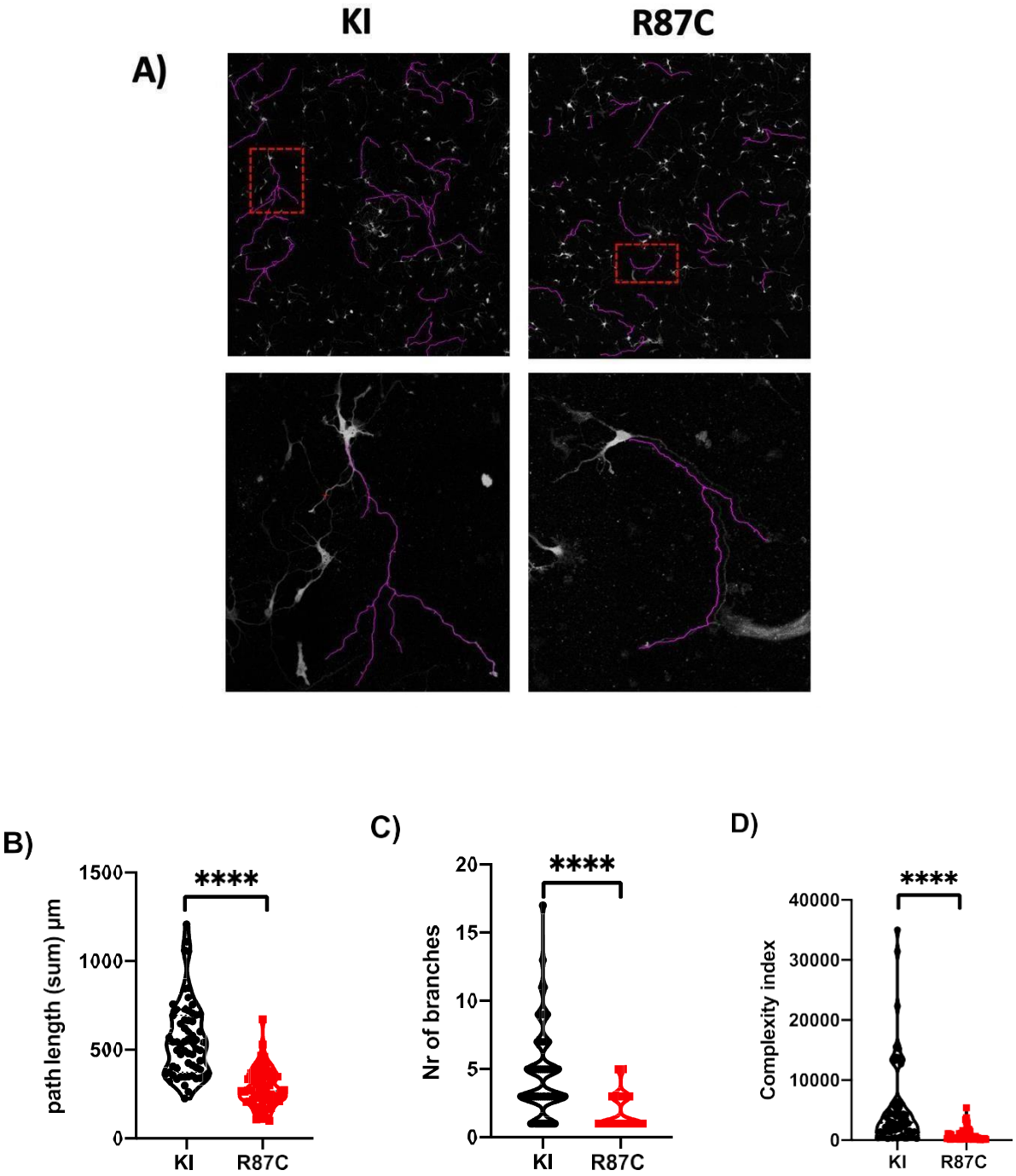

*Figure 4.14: A) Axon tracing of hippocampal culture at DIV3 by Simple Neurite Tracing in purple (Top). The complexity of axonal arborization was determined by analysing the total length of axons the number of branches, and the complexity index. (Nr = 63 (KI), 63 (R87C), Unpaired T-test: ****<0.0001) (Figure B,C,D).*

These findings strongly indicate that the R87C mutation may affects the process of axonal maturation, at least in early stages in *in vitro* development. However, additional research is necessary to clarify how this mutation influences this process and to uncover the underlying molecular mechanisms.

3.12 Study of spine frequency of hippocampal primary neurons

Spinogenesis is a dynamic process and essential for a correct neurotransmission, as well as for the formation of synapsis, and overall, for the neuroplasticity. This process relies in quickly rearrangement of actin dynamics which, on demand can rearrange to give shape to different types of spines after neurochemical stimuli. Indeed, dendritic spines are highly dynamic membranous protrusions on postsynaptic dendrites, which have a rich F-actin cytoskeleton (Shah and Rossie, 2018). Pathania and collaborators identified that both CYFIP1 and CYFIP2 are localized predominantly in dendric spines specifically in excitatory postsynaptic mature neurons suggesting an important role of these protein in this process. (Pathania et al., 2014). Moreover, Han and collaborators found out that mice with CYFIP2 haploinsufficiency displayed alterations in cortical dendritic spine maturation (Han et al., 2014). Also, Cyfip2 heterozygous mice exhibit abnormalities in the morphology of spines in adult CA1 pyramidal neurons. Given the importance of CYFIP2 in spinogenesis we aimed to study this process by employing our model of primary hippocampal neurons. Neuronal cells were cultured for 17 days, a timing considered sufficient for spine structures to reach maturity and functionality. During this period, both endogenous CYFIP1 and CYFIP2 were knocked down using lentiviral shRNA, while exogenous CYFIP2 KI was continuously expressed through lentiviral transduction. Afterward, the cells were fixed, and immunofluorescence staining with an α-HA antibody was carried out to visualize transgene expression. Using confocal microscopy, a GFP signal was captured from the cells, which was co-expressed with the shRNA. This signal served not only as a marker of the silencing of endogenous CYFIP2 but also it was useful to reconstruct the morphology of the neurons and assess the frequency of spines. For each experimental group, at least 15 dendrites were analysed. The number of spines in each secondary dendrite was manually counted by using Fiji Software

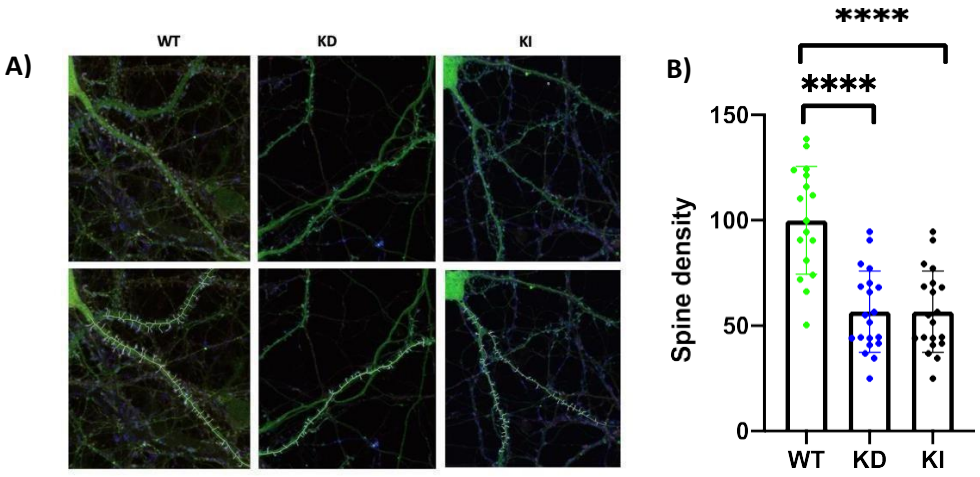

*Figure 4.15: A) Image of dendrites from hippocampal cells at DIV18, captured by confocal microscopy. The GFP protein signal, visible in green, marks the downregulation of CYFIP2. At the bottom, the dendrite reconstruction is shown in grey, with spine structures in blue. B) The graph represents the spine frequency of WT, KD, and KI cell populations (Nr=20 for WT, N = 18 for KD, Nr =18 for KI). (Tukey's multiple comparisons test ****< 0.0001).*

In this experiment, we observed a significant decrease in dendritic spine frequency in neurons with KD of CYFIP1 and CYFIP2 compared to WT. Surprisingly, a similar decrease was also observed in KI neurons, which was unexpected.

We then conducted the same experiment to investigate spinogenesis in the presence of the R87C mutation. As before, both CYFIP1 and CYFIP2 were knocked down using lentiviral shRNA, while R87C expression was maintained via lentiviral transduction. The cells were fixed, and immunofluorescence staining with an α-HA antibody was performed to visualize the transgene. Confocal microscopy was used to detect a GFP signal, co-expressed with the shRNA, which served as an indicator of CYFIP2 silencing. Additionally, this GFP signal helped in reconstructing neuronal morphology and evaluating spine frequency. For each condition, at least 15 dendrites were analyzed, and spine counts on secondary dendrites were manually performed using Fiji Software.

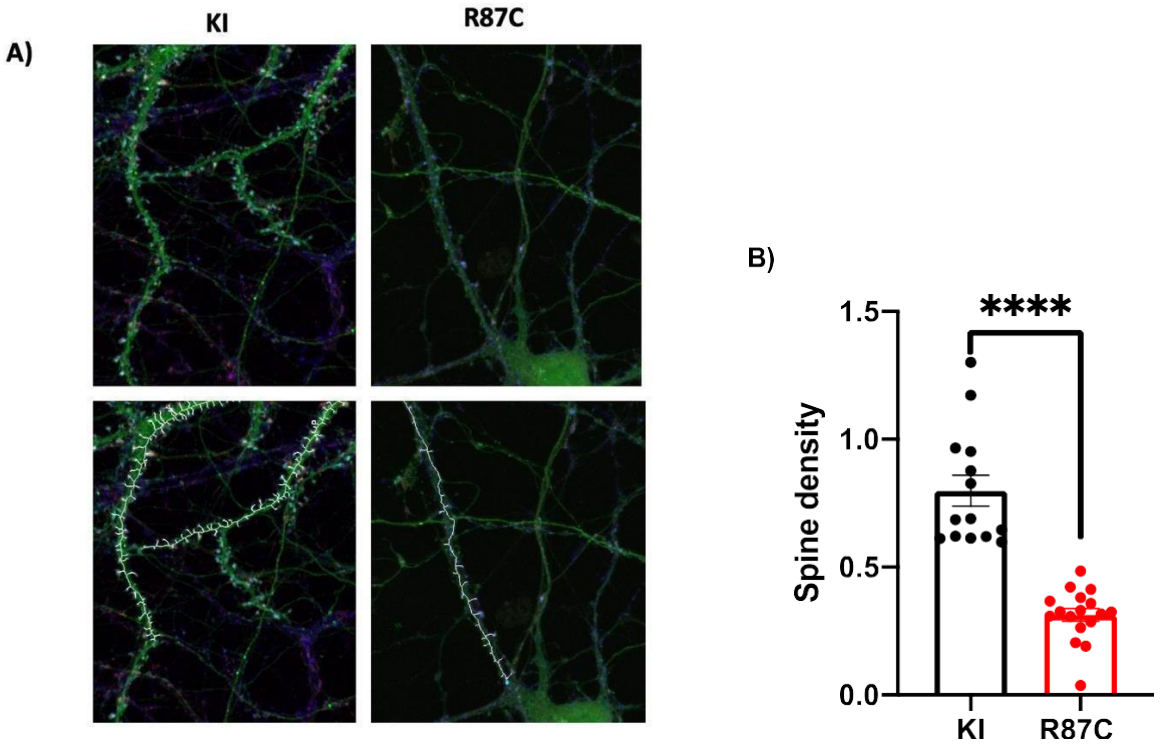

*Figure 4.16: A) Image of dendrites from hippocampal cells at DIV18, captured by confocal microscopy. The GFP protein signal, visible in green, marks the down-regulation of CYFIP2. At the bottom, the dendrite reconstruction is shown in grey, with spine structures in blue. B) The graph represents the spine frequency of KI and R87C cell populations (N = 17 for KI, N = 18 for R87C). (Unpaired T-test, ****< 0.0001).*

In this experiment, we observed a significant reduction in the number of spines in neurons carrying the CYFIP2 R87C mutation compared to the CYFIP2 KI neurons. These findings highlight the pivotal role of CYFIP2 in spinogenesis and suggest that this process may be impaired by mutated R87C variant. Taken together, these data indicate that CYFIP2 is crucial for proper spine formation, and the R87C mutation could potentially disrupt actin dynamics, leading to defects in spine morphology and potentially impairing synaptic function.

5. DISCUSSION AND CONCLUSION

So far, CYFIP1 and CYFIP2, both members of the WRC complex, were initially identified as binding partners of the FMRP protein, suggesting a role for both CYFIP1 and CYFIP2 in Fragile X Syndrome, a debilitating neurodevelopmental disorder. Since then, both proteins have been the focus of numerous studies, attributing their roles to a broader range of diseases, from neurological disorders to, more recently, cancer.

It is well established that the CYFIP1 and CYFIP2 proteins, key components of the WRC complex, act as a hub connecting signals from the plasma membrane to actin dynamics. Indeed, in its inactive state, the WRC complex is localized in the cytosol (Kage et al., 2022). Upon receiving signals, typically triggered by growth factors, the entire complex is recruited to specific membrane regions to promote actin polymerization by activating the Arp2/3 complex. The small GTPase Rac1, in its active GTP-bound form (Rac-GTP), is the primary trigger for WRC activation. Rac-GTP interacts with two binding sites on the WRC, designated as sites A and D, located within the CYFIP2 structure (or its paralog CYFIP1). This binding induces a series of conformational changes in the WRC, releasing the VCA domain (a segment involved in activating the Arp2/3 complex). Once released, the VCA domain activates the Arp2/3 complex, leading to actin polymerization. Throughout this process, CYFIP2 (or its paralog CYFIP1) plays a fundamental role. On a microscale level, dysfunction at this point has been associated with several alterations, as proper actin polymerization and depolymerization are affected. However, this is an oversimplification, as the role of this protein extends beyond its function within the WRC complex. CYFIP2 is also actively involved in local mRNA regulation, particularly in neurons, where it has the highest expression levels compared to other tissues. It is believed that there is a dynamic balance, with part of CYFIP2 localized within the WRC complex and another fraction regulating different processes on demand.

Two recent studies have independently reported hotspot de novo variants at the ARG87 position in the CYFIP2 gene among patients diagnosed with Early Infantile Epileptic Encephalopathy (EIEE) (Nakashima et al., 2018; Zhong et al., 2019). The pioneering study by Nakashima and colleagues in 2018 was the first to establish a direct link between CYFIP2 mutations and EIEE. In this comprehensive investigation, a cohort of 489 individuals with various subtypes of EIEE was analyzed. Within this group, the researchers identified three distinct de novo variants at the Arg87 codon (Arg87Leu, Arg87Cys, and Arg87Pro) in four unrelated patients diagnosed with West syndrome, highlighting the potential significance of this residue as a mutational hotspot.

Since the discovery of these de novo mutations at codon R87 by Nakashima and colleagues, significant progress has been made in exploring the role of these variants in the underlying mechanisms of EIEE. Being CYFIP2 protein a crucial component of the WAVE regulatory complex (WRC), alterations at this critical site might disrupt actin remodelling, affecting multiple cellular processes such as cell shape, movement, and synaptic function. This disruption may help explain the severe neurological manifestations observed in affected patients.

In particular, the R87C variant, one of the three identified mutations and object of our study, has been associated with the most severe clinical outcomes. Patients carrying the R87C mutation typically exhibit profound neurological symptoms and are often diagnosed with Ohtahara syndrome or West syndrome, both characterized by early onset, treatment-resistant seizures, and poor developmental prognosis. (Ohtahara et al., 1987) This variant's severe impact underscores the pathogenic potential of mutations at the R87 site and suggests that it plays a pivotal role in the pathophysiology of these early-onset epileptic disorders.

At the molecular level, the mutation of this protein leads to the substitution of the positively charged arginine amino acid with cysteine, which has a neutral charge. Chemically, positively charged amino acids are involved in electrostatic interactions as well as hydrogen bonding, both of which are critical for protein folding and spatial conformation. In fact, the loss of positive charge can disrupt local electrostatic interactions, destabilize the protein's structure, or interfere with binding sites for negatively charged molecules. Arginine often plays a role in stabilizing protein structures through salt bridges or hydrogen bonds (Chakkalakal et al., 2018). The replacement with cysteine could lead to a loss of these stabilizing interactions, resulting in local misfolding or a destabilized protein conformation.

The destabilization caused by the R87C variant has also been associated with lower levels of CYFIP2 protein expression (Zhang, Lee and Han, 2019; Kang et al., 2023). Han and colleagues observed a decrease in CYFIP2 expression in heterozygous KO mice. Notably, the R87C variant triggers the formation of CYFIP2 aggregates or clusters. The accumulation of these clusters likely engages the proteostasis machinery, such as the ubiquitin-proteasome system or autophagy pathways, to degrade the misfolded or aggregated proteins (Zhang, Lee and Han, 2019). We observed a similar outcome in our in vitro model represented by HEK293T cells, which showed CYFIP2, despite transfecting the same amount of plasmid carrying either the mutation variant or the WT protein. Further investigation revealed that this reduction in protein expression was due to increased levels of degradation. These results are consistent with other in vivo studies where reduced protein expression has been observed, likely because of accelerated degradation (Zhang, Lee and Han, 2019). It is probable that the formation of CYFIP2 clusters triggers activation of the ubiquitin-proteasome system, which helps clear the dysfunctional protein, leading to an overall reduction in CYFIP2 levels. This process may contribute to the pathophysiology associated with the mutation.

Beyond the destabilization caused by increased susceptibility to degradation due to the amino acid substitution, the mutated version of this protein also alters its functionality in the context of the WRC. In fact, an increase in its activity has been observed, even under basal conditions. Souza and colleague 2022, hypothesised that mutated variant R87C lead to a constant activation of the entire complex, even in the absence of external stimulation. Indeed, crystallography studies showed that hydrogen bonds normally presented in R87 residue with E62A and E689 are lost in CYFIP2 R87C models leading to a destabilization of the entire complex (Biembengut et al., 2022)

In our in vitro model represented by the neuroblastoma cell line, we first observed actin disorganization in the KO cells compared to the WT cells. Subsequently, in further analyses, we aimed to define the role of CYFIP2 as well as the mutated version, R87C, by measuring a set of parameters directly associated with actin dynamics and, consequently, with the activation of the WRC complex.

Our analysis revealed substantial differences across all measured parameters when comparing the WT and KO SH-SY5Y cell lines, as well as between the KO and KI models. Specifically, the KO cells displayed a significant increase in cell area, suggesting an altered cellular morphology due to the absence of CYFIP2. Interestingly, this enlargement of cell size was reversed in the KI model,

indicating that the introduced CYFIP2 was able to rescue the phenotype. The same results were observed for the aspect ratio, which reflects the elongation and overall shape of the cells, suggesting that CYFIP2 plays a critical role in maintaining proper cell geometry.

Additionally, integrated density, a parameter used to assess the levels of f-actin, was also significantly elevated in KO cells and returned to near-normal levels in the KI model. This suggests that the absence of CYFIP2 disrupts actin organization, leading to an accumulation of f-actin, which impacts the overall cellular architecture. The restoration of these parameters in the KI model supports the idea that CYFIP2 is vital for regulating actin dynamics, which in turn governs cell shape, size, and structural integrity. Overall, these findings point to a fundamental role of CYFIP2 in determining cell morphology, highlighting its importance in actin filament regulation and suggesting that disruptions in its function can lead to significant changes in cellular structure and behaviour.

The same analysis was repeated to define in this case the role of R87C. In this experiment, we identified significant differences between the KI model and the R87C variant in terms of cell area and integrated density. Notably, both parameters showed a marked increase in the R87C variant, like what was observed in the KO model. This suggests that the R87C mutation, like the complete loss of CYFIP2 in the KO model, leads to disrupted cellular regulation, resulting in enlarged cell size and increased f-actin content. On the other hand, when examining the aspect ratio, no significant differences were detected between the different cell populations, indicating that the elongation or overall shape of the cells remained unchanged despite the variations in size and actin density.

Given the high expression of CYFIP2 in the brain (Zhang et al., 2019) and its critical role in early neurodevelopment, we aimed to assess cellular differentiation in our in vitro model represented by neuroblastoma cell line. This process is fundamental during the initial stages of neurodevelopment, as it involves extensive recruitment and reorganization of the actin cytoskeleton. Actin dynamics are crucial for the morphological changes required during differentiation, including the formation of neurites and the establishment of cell polarity, making this an important aspect to investigate in the context of CYFIP2 function. In this experiment, CYFIP2 KO cells failed to develop characteristic neurite-like structures following differentiation, unlike the WT cells. However, this defect was fully corrected in the KI model, where neurite formation was restored. These findings underscore the essential role of CYFIP2 in neuronal differentiation.

Similar to KO model, the R87C mutant cell population did not develop the characteristic neurite-like structures observed during differentiation. This inability to form neurites suggests that the R87C mutation may have disruptive effect on the cellular mechanisms required for proper differentiation. Given the crucial role of actin dynamics in this process and the involvement of CYFIP2 in actin regulation, it is possible that the R87C mutation impairs cytoskeletal organization, affecting the cell's ability to extend neurites. However, additional research is needed to better understand the underlying mechanisms by which the R87C variant interferes with differentiation, as the exact pathways remain unclear.

To gain a deeper understanding of the role of CYFIP2 and the R87C mutation in neuronal function, we next utilized primary neuronal cell cultures derived from murine embryos. This approach allowed us to study the direct effects of CYFIP2 and the R87C variant on neuronal development. It has been widely showed in literature the involvement of CYFIP2 in the growth and sorting of retinal ganglion cells axons (Cioni *et al.*, 2018). For this reason, we initially focused on the early stages of neuronal maturation, analysing neuronal axon length and complexity during the first days of *in vitro* neuronal development. By evaluating these parameters in primary murine hippocampal neurons, we observed a reduction in terms of axon length, number of branches as well as complexity index in the KD neurons compared to WT. Interestingly a reduction of these parameters was observed also in KI cells. This discrepancy may be due to a series of mechanisms that doesn't permit the exogenous protein to fully exhibit the proper action in the same manner as WT version. The reasons may include issues with localization or differences in post-translational modifications (e.g., phosphorylation, ubiquitination) between the KI and WT proteins, which could impact their function, stability, or interactions with other cellular components. Additionally, in WT cells, the gene's native chromosomal context includes regulatory elements like enhancers and promoters that tightly control its expression. However, exogenous knock-in typically bypasses these elements, often leading to altered expression levels or incorrect timing compared to the endogenous gene.

On the other hand, upon evaluating axon length, number of branches and the complexity index in both KI and R87C neuronal populations, we observed a significant difference between them. Specifically, neurons expressing the R87C mutation variant exhibited impaired axon development compared to the KI cells. More precisely, we observed that the axons of mutated neurons were significantly shorter, with fewer branches, leading to a lower overall complexity index. In this case the technical differences between KI, CYFIP2 and R87C populations (differences in the CYFIP2

expression) are somehow normalized. This suggests that the observed impairments in axon development and complexity are not due to technical artifacts or differences in cell culture conditions, but rather are directly attributable to the mutation itself. These findings indicate that the R87C mutation has a profound impact on neuronal morphology, specifically impairing axon elongation and branching, which may have important implications for understanding the role of CYFIP2 in neuronal development and function.

Dendritic spines are highly dynamic membranous protrusions on postsynaptic dendrites, which are enriched in the f-actin cytoskeleton and play a crucial role in synaptic plasticity and signal transmission (Shah and Rossie, 2018). Furthermore, Cyfip2 is known to be highly expressed in these structures, where it likely contributes to their development and function (Pathania *et al.*, 2014). Given the critical role of CYFIP2 in dendritic spine structure and function, we aimed to extend our study by evaluating spine density across different neuronal populations, including WT, KD, and KI, and subsequently comparing these to the KI and R87C neuronal populations. In our analysis, we observed a significant reduction in the overall number of dendritic spines in KD cells compared to WT. Interestingly, a similar reduction in spine density was also observed in KI cells, which may be attributed to the factors I mentioned earlier regarding the technical differences in KI cell generation or the impact of CYFIP2 expression.

More intriguingly, when comparing the KI and R87C neuronal populations, we observed a significant decrease in spine density in neurons expressing the R87C mutation. These results suggest a potential impairment in spinogenesis associated with the mutation, which aligns with findings from existing literature. For instance, CYFIP2 haploinsufficiency in mice has been shown to result in altered cortical dendritic spine maturation (Han et al., 2014). Additionally, CYFIP2 heterozygous mice exhibit abnormalities in spine morphology, particularly in adult CA1 pyramidal neurons. These findings support the idea that mutations in CYFIP2, such as R87C, could impair spine development and potentially affect synaptic function and plasticity.

In conclusion, all these data taken together suggest that CYFIP2 plays a vital role in regulating cell shape and size through its involvement in actin dynamics, particularly in highly polarized cells such as neurons. On the other hand, the R87C mutation aligns with one of the most widely accepted hypotheses in the literature, which posits that its pathogenicity is mostly due to reduced interaction with the WAVE protein, which is a key point into the WRC. This weakened interaction with WAVE

leads to a loss of autoinhibition, resulting in both destabilization of the CYFIP2 protein itself and aberrant activation of the WRC complex, even in the absence of stimuli. This hypothesis was supported by our findings, as we observed dysregulation in terms of f-actin specifically in SH-SY5Y cells suggesting a constant and aberrant activation of WRC. Additionally, we noted structural alterations where fine-tuning of actin rearrangement is crucial, such as in processes like axon growth and spinogenesis.

6. BIBLIOGRAPHY:

- Abdul-Manan, N. *et al.* (1999) 'Structure of Cdc42 in complex with the GTPase-binding domain of the "Wiskott-Aldrich syndrome" protein', *Nature*, 399(6734). Available at: https://doi.org/10.1038/20726.
- Abekhoukh, S. *et al.* (2017) 'New insights into the regulatory function of CYFIP1 in the context of WAVE- and FMRP-containing complexes', *DMM Disease Models and Mechanisms*, 10(4). Available at: https://doi.org/10.1242/dmm.025809.
- Arshadi, C. *et al.* (2021) 'SNT: a unifying toolbox for quantification of neuronal anatomy', *Nature Methods*, 18(4). Available at: https://doi.org/10.1038/s41592-021-01105-7.
- Auvin, S., Cilio, M.R. and Vezzani, A. (2016) 'Current understanding and neurobiology of epileptic encephalopathies', *Neurobiology of Disease*. Available at: https://doi.org/10.1016/j.nbd.2016.03.007.
- Begemann, A. *et al.* (no date) 'New insights into the clinical and molecular spectrum of the novel CYFIP2-related neurodevelopmental disorder and impairment of the WRC-mediated actin dynamics', *GENETICS in MEDICINE* [Preprint]. Available at: https://doi.org/10.1038/s41436.
- Bergert, M. *et al.* (no date) 'Cell mechanics control rapid transitions between blebs and lamellipodia during migration'. Available at: https://doi.org/10.1073/pnas.1207968109/-/DCSupplemental.
- Biembengut, Í. V. *et al.* (2022) 'Molecular Dynamics of CYFIP2 Protein and Its R87C Variant Related to Early Infantile Epileptic Encephalopathy', *International Journal of Molecular Sciences*, 23(15). Available at: https://doi.org/10.3390/ijms23158708.
- Biembengut, Í.V. *et al.* (2021) 'Cytoplasmic FMR1 interacting protein (CYFIP) family members and their function in neural development and disorders', *Molecular Biology Reports*. Available at: https://doi.org/10.1007/s11033-021-06585-6.
- Blanchoin, L. *et al.* (2014) 'Actin dynamics, architecture, and mechanics in cell motility', *Physiological Reviews*, 94(1). Available at: https://doi.org/10.1152/physrev.00018.2013.

- Bonini, D. *et al.* (2015) 'Chronic glutamate treatment selectively modulates AMPA RNA editing and ADAR expression and activity in primary cortical neurons', *RNA Biology*, 12(1). Available at: https://doi.org/10.1080/15476286.2015.1008365.
- Butler, M.G. (2017) 'Clinical and genetic aspects of the 15q11.2 BP1–BP2 microdeletion disorder', *Journal of Intellectual Disability Research*, 61(6), pp. 568–579. Available at: https://doi.org/10.1111/jir.12382.
- Campellone, K.G. and Welch, M.D. (2010) 'A nucleator arms race: Cellular control of actin assembly', *Nature Reviews Molecular Cell Biology*, pp. 237–251. Available at: https://doi.org/10.1038/nrm2867.
- Chakkalakal, S.A. *et al.* (2018) 'Impact of arginine to cysteine mutations in collagen ii on protein secretion and cell survival', *International Journal of Molecular Sciences*, 19(2). Available at: https://doi.org/10.3390/ijms19020541.
- Charras, G.T. *et al.* (2005) *Non-equilibration of hydrostatic pressure in blebbing cells*, *Nature*.
- Chen, Z. *et al.* (2010) 'Structure and control of the actin regulatory WAVE complex', *Nature*, 468(7323). Available at: https://doi.org/10.1038/nature09623.
- Cheng, Y. *et al.* (2017) 'De novo SCN2A mutation in a Chinese infant with severe early-onset epileptic encephalopathy, bronchopulmonary dysplasia, and adrenal hypofunction', *International Journal of Clinical and Experimental Pathology*, 10(10).
- Cioni, J.M. *et al.* (2018) 'Axon-Axon Interactions Regulate Topographic Optic Tract Sorting via CYFIP2-Dependent WAVE Complex Function', *Neuron*, 97(5). Available at: https://doi.org/10.1016/j.neuron.2018.01.027.
- Clifton, N.E. *et al.* (2020) 'FMRP and CYFIP1 at the Synapse and Their Role in Psychiatric Vulnerability', *Complex Psychiatry*. S. Karger AG, pp. 5–19. Available at: https://doi.org/10.1159/000506858.
- Concordet, J.P. and Haeussler, M. (2018) 'CRISPOR: Intuitive guide selection for CRISPR/Cas9 genome editing experiments and screens', *Nucleic Acids Research*, 46(W1). Available at: https://doi.org/10.1093/nar/gky354.
- Contreras, E.G. *et al.* (2018) 'Dynamic Notch signalling regulates neural stem cell state progression in the Drosophila optic lobe 11 Medical and Health Sciences 1109 Neurosciences', *Neural Development*, 13(1). Available at: https://doi.org/10.1186/s13064-018-0123-8.

- Daniel, C., Behm, M. and Öhman, M. (2015) 'The role of Alu elements in the cis-regulation of RNA processing', *Cellular and Molecular Life Sciences*. Available at: https://doi.org/10.1007/s00018-015-1990-3.
- DeRubeis, S. *et al.* (2013) 'CYFIP1 coordinates mRNA translation and cytoskeleton remodeling to ensure proper dendritic Spine formation', *Neuron*, 79(6), pp. 1169–1182. Available at: https://doi.org/10.1016/j.neuron.2013.06.039.
- Domínguez-Iturza, N. *et al.* (2019) 'The autism- and schizophrenia-associated protein CYFIP1 regulates bilateral brain connectivity and behaviour', *Nature Communications*, 10(1). Available at: https://doi.org/10.1038/s41467-019-11203-y.
- Dziunycz, P.J. *et al.* (2017) 'CYFIP1 is directly controlled by NOTCH1 and down-regulated in cutaneous squamous cell carcinoma', *PLoS ONE*, 12(4). Available at: https://doi.org/10.1371/journal.pone.0173000.
- Egger, B., Gold, K.S. and Brand, A.H. (2010) 'Notch regulates the switch from symmetric to asymmetric neural stem cell division in the Drosophila optic lobe', *Development*, 137(18). Available at: https://doi.org/10.1242/dev.051250.
- Gautreau, A. *et al.* (2004) 'Purification and architecture of the ubiquitous Wave complex', *Proceedings of the National Academy of Sciences of the United States of America*, 101(13). Available at: https://doi.org/10.1073/pnas.0400628101.
- Ghosh, A. *et al.* (2020) 'Alzheimer's disease-related dysregulation of mRNA translation causes key pathological features with ageing', *Translational Psychiatry*, 10(1). Available at: https://doi.org/10.1038/s41398-020-00882-7.
- Habela, C.W. *et al.* (2020) 'Persistent CyFIP1 expression is required to maintain the adult subventricular zone neurogenic niche', *Journal of Neuroscience*, 40(10). Available at: https://doi.org/10.1523/JNEUROSCI.2249-19.2020.
- Han, K. *et al.* (2014) 'Fragile X-like behaviors and abnormal cortical dendritic spines in Cytoplasmic FMR1-interacting protein 2-mutant mice', *Human Molecular Genetics*, 24(7). Available at: https://doi.org/10.1093/hmg/ddu595.
- Hancock, E.C., Osborne, J.P. and Edwards, S.W. (2013) 'Treatment of infantile spasms', *Cochrane Database of Systematic Reviews*. Available at: https://doi.org/10.1002/14651858.CD001770.pub3.

- Hoeffer, C.A. *et al.* (2012) 'Altered mTOR signaling and enhanced CYFIP2 expression levels in subjects with fragile X syndrome', *Genes, Brain and Behavior*, 11(3), pp. 332–341. Available at: https://doi.org/10.1111/j.1601-183X.2012.00768.x.
- Hromadkova, L. *et al.* (2020) 'Brain-derived neurotrophic factor (BDNF) promotes molecular polarization and differentiation of immature neuroblastoma cells into definitive neurons', *Biochimica et Biophysica Acta - Molecular Cell Research*, 1867(9). Available at: https://doi.org/10.1016/j.bbamcr.2020.118737.
- Jain, P., Sharma, S. and Tripathi, M. (2013) 'Diagnosis and Management of Epileptic Encephalopathies in Children', *Epilepsy Research and Treatment*, 2013. Available at: https://doi.org/10.1155/2013/501981.
- Jamain, S. *et al.* (2003) 'Mutations of the X-linked genes encoding neuroligins NLGN3 and NLGN4 are associated with autism', *Nature Genetics*, 34(1). Available at: https://doi.org/10.1038/ng1136.
- Kage, F. *et al.* (2022) 'Lamellipodia-like actin networks in cells lacking WAVE regulatory complex', *Journal of Cell Science*, 135(15). Available at: https://doi.org/10.1242/jcs.260364.
- Kanellopoulos, A.K. *et al.* (2020) 'Aralar Sequesters GABA into Hyperactive Mitochondria, Causing Social Behavior Deficits', *Cell*, 180(6), pp. 1178-1197.e20. Available at: https://doi.org/10.1016/j.cell.2020.02.044.
- Kang, M. *et al.* (2023) 'CYFIP2 p.Arg87Cys Causes Neurological Defects and Degradation of CYFIP2', *Annals of Neurology*, 93(1), pp. 155–163. Available at: https://doi.org/10.1002/ana.26535.
- Kato, M. *et al.* (2004) 'Mutations of ARX Are Associated with Striking Pleiotropy and Consistent Genotype-Phenotype Correlation', *Human Mutation*. Available at: https://doi.org/10.1002/humu.10310.
- Keane, T.M. *et al.* (2011) 'Mouse genomic variation and its effect on phenotypes and gene regulation', *Nature*, 477(7364). Available at: https://doi.org/10.1038/nature10413.
- Kim, G.H. *et al.* (2020) 'Altered presynaptic function and number of mitochondria in the medial prefrontal cortex of adult Cyfip2 heterozygous mice', *Molecular Brain*, 13(1). Available at: https://doi.org/10.1186/s13041-020-00668-4.
- Kirkpatrick, S.L. *et al.* (2017) 'Cytoplasmic FMR1-Interacting Protein 2 Is a Major Genetic Factor Underlying Binge Eating', *Biological Psychiatry*, 81(9). Available at: https://doi.org/10.1016/j.biopsych.2016.10.021.

- Kobayashi, K. *et al.* (1998) 'p140Sra-1 (specifically Rac1-associated protein) is a novel specific target for Rac1 small GTPase', *Journal of Biological Chemistry*, 273(1). Available at: https://doi.org/10.1074/jbc.273.1.291.
- Koestler, S.A. *et al.* (2013) 'Arp2/3 complex is essential for actin network treadmilling as well as for targeting of capping protein and cofilin', *Molecular Biology of the Cell*, 24(18). Available at: https://doi.org/10.1091/mbc.E12-12-0857.
- Kumar, V. *et al.* (2013) 'C57BL/6N mutation in cytoplasmic FMRP interacting protein 2 regulates cocaine response', *Science*, 342(6165), pp. 1508–1512. Available at: https://doi.org/10.1126/science.1245503.
- Kwak, S., Nishimoto, Y. and Yamashita, T. (2008) 'Newly identified ADAR-mediated A-to-I editing positions as a tool for ALS research', *RNA Biology*. Available at: https://doi.org/10.4161/rna.6925.
- Lappalainen, P. *et al.* (2022) 'Biochemical and mechanical regulation of actin dynamics', *Nature Reviews Molecular Cell Biology*. Available at: https://doi.org/10.1038/s41580-022-00508-4.
- Lee, Y. *et al.* (2020) 'Epilepsy- and intellectual disability-associated CYFIP2 interacts with both actin regulators and RNA-binding proteins in the neonatal mouse forebrain', *Biochemical and Biophysical Research Communications*, 529(1), pp. 1–6. Available at: https://doi.org/10.1016/j.bbrc.2020.05.221.
- Lin, J. *et al.* (2020) 'circCYFIP2 Acts as a Sponge of miR-1205 and Affects the Expression of Its Target Gene E2F1 to Regulate Gastric Cancer Metastasis', *Molecular Therapy Nucleic Acids*, 21, pp. 121–132. Available at: https://doi.org/10.1016/j.omtn.2020.05.007.
- Malik, S.I. *et al.* (2013) 'Epilepsy surgery for early infantile epileptic encephalopathy (ohtahara syndrome)', *Journal of Child Neurology*, 28(12). Available at: https://doi.org/10.1177/0883073812464395.
- Mayne, M. *et al.* (2004) 'CYFIP2 is highly abundant in CD4+ cells from multiple sclerosis patients and is involved in T cell adhesion', *European Journal of Immunology*, 34(4), pp. 1217–1227. Available at: https://doi.org/10.1002/eji.200324726.
- Nakashima, M. *et al.* (2018) 'De novo hotspot variants in CYFIP2 cause early-onset epileptic encephalopathy', *Annals of Neurology*, 83(4). Available at: https://doi.org/10.1002/ana.25208.

- Napoli, I. *et al.* (2008) 'The Fragile X Syndrome Protein Represses Activity-Dependent Translation through CYFIP1, a New 4E-BP', *Cell*, 134(6), pp. 1042–1054. Available at: https://doi.org/10.1016/j.cell.2008.07.031.
- Nicholas, A. *et al.* (2010) 'Age-related gene-specific changes of A-to-I mRNA editing in the human brain', *Mechanisms of Ageing and Development*, 131(6). Available at: https://doi.org/10.1016/j.mad.2010.06.001.
- Noroozi, R. *et al.* (2018) 'Cytoplasmic FMRP interacting protein 1/2 (CYFIP1/2) expression analysis in autism', *Metabolic Brain Disease*, 33(4). Available at: https://doi.org/10.1007/s11011-018-0249-8.
- Oakes, P.W. *et al.* (2018) 'Lamellipodium is a myosin-independent mechanosensor', *Proceedings of the National Academy of Sciences of the United States of America*, 115(11), pp. 2646–2651. Available at: https://doi.org/10.1073/pnas.1715869115.
- Oguro-Ando, A. *et al.* (2015) 'Increased CYFIP1 dosage alters cellular and dendritic morphology and dysregulates mTOR', *Molecular Psychiatry*, 20(9), pp. 1069–1078. Available at: https://doi.org/10.1038/mp.2014.124.
- Ohtahara, S. *et al.* (1987) 'The early-infantile epileptic encephalopathy with suppression-burst: Developmental aspects', *Brain and Development*, 9(4). Available at: https://doi.org/10.1016/S0387-7604(87)80110-9.
- Ostrander, B.E.P. *et al.* (2018) 'Whole-genome analysis for effective clinical diagnosis and gene discovery in early infantile epileptic encephalopathy', *npj Genomic Medicine*, 3(1). Available at: https://doi.org/10.1038/s41525-018-0061-8.
- Ozaki, T. and Nakagawara, A. (2011) 'Role of p53 in cell death and human cancers', *Cancers*, pp. 994–1013. Available at: https://doi.org/10.3390/cancers3010994.
- Paluch, E.K. and Raz, E. (2013) 'The role and regulation of blebs in cell migration', *Current Opinion in Cell Biology*, pp. 582–590. Available at: https://doi.org/10.1016/j.ceb.2013.05.005.
- Pan, L. *et al.* (2004) 'The Drosophila fragile X gene negatively regulates neuronal elaboration and synaptic differentiation', *Current Biology*, 14(20). Available at: https://doi.org/10.1016/j.cub.2004.09.085.
- Pathania, M. *et al.* (2014) 'The autism and schizophrenia associated gene CYFIP1 is critical for the maintenance of dendritic complexity and the stabilization of mature spines', *Translational Psychiatry*, 4. Available at: https://doi.org/10.1038/tp.2014.16.

- Phillips, M. and Pozzo-Miller, L. (2014) 'Dendritic spine dysgenesis in autism related disorders', *Neuroscience Letters*. Available at: https://doi.org/10.1016/j.neulet.2015.01.011.
- Poke, G. *et al.* (2023) 'Epidemiology of Developmental and Epileptic Encephalopathy and of Intellectual Disability and Epilepsy in Children', *Neurology*, 100(13). Available at: https://doi.org/10.1212/WNL.0000000000206758.
- Radaelli, G. *et al.* (2018) 'Causes of mortality in early infantile epileptic encephalopathy: A systematic review', *Epilepsy and Behavior*. Available at: https://doi.org/10.1016/j.yebeh.2018.05.015.
- Ran, F.A. *et al.* (2013) 'Genome engineering using the CRISPR-Cas9 system', *Nature Protocols*, 8(11). Available at: https://doi.org/10.1038/nprot.2013.143.
- 'Reply to "Reduced CYFIP2 Stability by Arg87 Variants Causing Human Neurological Disorders" - Nakashima - 2019 - Annals of Neurology - Wiley Online Library' (no date).
- Rottner, K., Stradal, T.E.B. and Chen, B. (2021) *WAVE regulatory complex*.
- Sayad, A. *et al.* (2018) 'Expression Analysis of CYFIP1 and CAMKK2 Genes in the Blood of Epileptic and Schizophrenic Patients', *Journal of Molecular Neuroscience*, 65(3). Available at: https://doi.org/10.1007/s12031-018-1106-2.
- Schacher, S. (1992) 'Culturing nerve cells', *Biological Psychology*, 33(2–3). Available at: https://doi.org/10.1016/0301-0511(92)90040-2.
- Schaks, M., Giannone, G. and Rottner, K. (2019) 'Actin dynamics in cell migration', *Essays in Biochemistry*, 63(5), pp. 483–495. Available at: https://doi.org/10.1042/EBC20190015.
- Scheffer, I.E. *et al.* (2017) 'ILAE classification of the epilepsies: Position paper of the ILAE Commission for Classification and Terminology', *Epilepsia*, 58(4). Available at: https://doi.org/10.1111/epi.13709.
- Schenck, A. *et al.* (2001) 'A highly conserved protein family interacting with the fragile X mental retardation protein (FMRP) and displaying selective interactions with FMRP-related proteins FXR1P and FXR2P', *Proceedings of the National Academy of Sciences of the United States of America*, 98(15). Available at: https://doi.org/10.1073/pnas.151231598.
- Schindelin, J. *et al.* (2012) 'Fiji: An open-source platform for biological-image analysis', *Nature Methods*. Available at: https://doi.org/10.1038/nmeth.2019.
- Shah, K. and Rossie, S. (2018) 'Tale of the Good and the Bad Cdk5: Remodeling of the Actin Cytoskeleton in the Brain', *Molecular Neurobiology*. Available at: https://doi.org/10.1007/s12035-017-0525-3.

- Da Silva Cardoso, J. *et al.* (2023) 'Clinical Role of Codon 87 of the CYFIP2 Gene in Early Infantile Epileptic Encephalopathy: A Clinical Case Description', *Cureus* [Preprint]. Available at: https://doi.org/10.7759/cureus.35323.
- Steffen, A. *et al.* (2006) 'Filopodia formation in the absence of functional WAVE- and Arp2/3-complexes', *Molecular Biology of the Cell*, 17(6), pp. 2581–2591. Available at: https://doi.org/10.1091/mbc.E05-11-1088.
- Steffen, A. *et al.* (2013) 'Rac function is crucial for cell migration but is not required for spreading and focal adhesion formation', *Journal of Cell Science*, 126(20). Available at: https://doi.org/10.1242/jcs.118232.
- Su, A.I. *et al.* (2004) 'A gene atlas of the mouse and human protein-encoding transcriptomes', *Proceedings of the National Academy of Sciences of the United States of America*, 101(16). Available at: https://doi.org/10.1073/pnas.0400782101.
- Suraneni, P. *et al.* (2012) 'The Arp2/3 complex is required for lamellipodia extension and directional fibroblast cell migration', *Journal of Cell Biology*, 197(2). Available at: https://doi.org/10.1083/jcb.201112113.
- Tiwari, S.S. *et al.* (2016) 'Alzheimer-related decrease in CYFIP2 links amyloid production to tau hyperphosphorylation and memory loss', *Brain*, 139(10), pp. 2751–2765. Available at: https://doi.org/10.1093/brain/aww205.
- Vesely, C. and Jantsch, M.F. (2021) 'An i for an a: Dynamic regulation of adenosine deamination-mediated rna editing', *Genes*. Available at: https://doi.org/10.3390/genes12071026.
- Wahlstedt, H. *et al.* (2009) 'Large-scale mRNA sequencing determines global regulation of RNA editing during brain development', *Genome Research*, 19(6), pp. 978–986. Available at: https://doi.org/10.1101/gr.089409.108.
- Yanai, I. *et al.* (2005) 'Genome-wide midrange transcription profiles reveal expression level relationships in human tissue specification', *Bioinformatics*, 21(5). Available at: https://doi.org/10.1093/bioinformatics/bti042.
- Zhang, Y., Lee, Y. and Han, K. (2019) 'Neuronal function and dysfunction of CYFIP2: From actin dynamics to early infantile epileptic encephalopathy', *BMB Reports*. The Biochemical Society of the Republic of Korea, pp. 304–311. Available at: https://doi.org/10.5483/BMBRep.2019.52.5.097.

- Zhong, M. *et al.* (2019) 'Early diagnosis improving the outcome of an infant with epileptic encephalopathy with cytoplasmic FMRP interacting protein 2 mutation: Case report and literature review', *Medicine*, 98(44), p. e17749. Available at: https://doi.org/10.1097/MD.0000000000017749.
- Zweier, M. *et al.* (2019) 'Spatially clustering de novo variants in CYFIP2, encoding the cytoplasmic FMRP interacting protein 2, cause intellectual disability and seizures', *European Journal of Human Genetics*, 27(5), pp. 747–759. Available at: https://doi.org/10.1038/s41431-018-0331-z.

7. LIST OF PUBBLICATIONS:

Pubblications in scientific journals:

1. Changes at glutamate tripartite synapsis in the prefrontal cortex of a new animal model of resilience/vulnerability to acute stress.
Bonifacino T, Mingardi J, Facchinetti R, Sala N, Frumento G, **Ndoj E**, Valenza M, Paoli C, Ieraci A, Torazza C, Balbi M, Guerinoni M, Muhammad N, Russo I, Milanese M, Scuderi C, Barbon A, Steardo L, Bonanno G, Popoli M, Musazzi L.

2. Transcriptional Profiling of Rat Prefronal Cortex after Acute Inescapable Footshock Stress.
Martini P, Mingardi J, Carini G, Mattevi S, **Ndoj E**, La Via L, Magri C, Gennarelli M, Russo I, Popoli M, Musazzi L, Barbon A.

3. Dopamine-Dependent Ketamine Modulation of Glutamatergic Synaptic Plasticity in the Prelimbic Cortex of Adult Rats Exposed to Acute stress.
Forti L, **Ndoj E**, Mingardi J, Secchi E, Bonifacino T, Schiavon E, Carini G, La Via L,Russo I Milanese M, Gennarelli M, Bonanno G, Popoli M, Barbon A, Musazzi

4. Functional and Molecular Changes in the Prefrontal Cortex of the Chronic Mild Stress Rat Model of Depression and Modulation by Acute Ketamine.
Mingardi J, **Ndoj E**, Bonifacino T, Misztak P, Bertoli M, La Via L, Torazza C, Russo I, Milanese M, Bonanno G, Popoli M, Barbon A, Musazzi L.

Papers in preparation:

1. K/E RNA editing of CYFIP2 regulates actin related neuronal development in vitro
Luca La Via, **Elona Ndoj**, Matteo Bertoli, Veronica Mutti, Giulia Carini, Alice Filippini, Federica Bono, Chiara Fiorentini, Isabella Russo, Alessandro Barbon.
2. Unraveling the role of CYFIP2 and R87C mutation in "in vitro" neurodevelopment
Elona Ndoj, Luca La Via, Matteo Bertoli, Alessandro Barbon.

Oral presentation at congresses

Elona Ndoj, Luca La Via, Jessica Mingardi, Laura Musazzi, Alessandro Barbon
Abstract: The role of α-synuclein in stress response and depression
Lake Como School of advanced studies (May 2022)

Abstract at congresses :

1. **Elona Ndoj**, Luca La Via, Jessica Mingardi, Laura Musazzi, Alessandro Barbon

Abstract: AMPA and NMDA receptors expression modifications in the PFC of rat model of PTSD and after ketamine treatment
New prospective in neuroscience: Research results of young Italian neuroscientists
University of Brescia (June 2022)

2. **Elona Ndoj**, Gaia Faustini, Luca La Via, Jessica Mingardi, Arianna Bellucci, Laura Musazzi, Alessandro Barbon

Abstract: The role of α-synuclein in stress response and depression
FENS regional meeting: Algarve, Portugal (May 2023)

3. **Elona Ndoj**, Luca La Via, Matteo Bertoli, Alessandro Barbon

Abstract: Cyfip2 and R87C mutation: Unraveling the role in neurodevelopmental disorders.
FENS Forum : Vienna, Austria (June 2024)

Acknowledgment:

I would like to express my sincere gratitude to the Department of Molecular and Translational Medicine (DMMT) and to everyone who supported me throughout my Ph.D. journey.
Special thanks to the best professor I could have ever asked for, Alessandro Barbon, for his guidance, unwavering support, and the invaluable knowledge he shared with me over these three years.
I am deeply thankful to Luca for his constant availability, patience, and invaluable guidance in my scientific work. His significant contributions have been crucial in shaping my Ph.D. journey from the very beginning. I extend my thanks to all the members of Lab 14 for their support throughout this process.
I also extend my sincere gratitude to Cesare Orlandi and his laboratory at the University of Rochester for providing me with the opportunity to broaden my academic horizons in the United States.

Immense thanks and heartfelt gratitude go to my family for their unwavering support and constant presence throughout my life.
I am also grateful to my friends who accompanied me on this journey, with special appreciation to my friend Antonio, whose encouragement at a critical moment was pivotal in starting this incredible and life-changing path.